Journal of Visualized Experiments

High-throughput analysis of optical mapping data using ElectroMap

--Manuscript Draft--

Article Type:	Invited Methods Article - JoVE Produced Video
Manuscript Number:	JoVE59663R2
Full Title:	High-throughput analysis of optical mapping data using ElectroMap
Keywords:	Cardiac Optical Mapping, Software, Electrophysiology, Arrythmia, Fluorescent Sensors, Action Potential, Calcium
Corresponding Author:	Davor Pavlovic University of Birmingham Birmingham, UNITED KINGDOM
Corresponding Author's Institution:	University of Birmingham
Corresponding Author E-Mail:	D.Pavlovic@bham.ac.uk
Order of Authors:	Christopher O'Shea
	Andrew P Holmes
	Ting Y Yu
	James Winter
	Simon P Wells
	Beth A Parker
	Dannie Fobian
	Daniel M Johnson
	Joao Correia
	Paulus Kirchhof
	Larissa Fabritz
	Kashif Rajpoot
	Davor Pavlovic
Additional Information:	
Question	**Response**
Please indicate whether this article will be Standard Access or Open Access.	Open Access (US$4,200)
Please indicate the **city, state/province, and country** where this article will be **filmed**. Please do not use abbreviations.	Birmingham, West Midlands, UK

TITLE:

High-Throughput Analysis of Optical Mapping Data Using ElectroMap

AUTHORS & AFFILIATIONS:

Christopher O'Shea[1,2,3], Andrew P Holmes[1,4], Ting Y Yu[1], James Winter[1], Simon P Wells[1], Beth A Parker[1], Dannie Fobian[1], Daniel M Johnson[1], Joao Correia[5], Paulus Kirchhof[1], Larissa Fabritz[1], Kashif Rajpoot[3], Davor Pavlovic[1]

[1]Institute of Cardiovascular Sciences, University of Birmingham, UK
[2]EPSRC Centre for Doctoral Training in Physical Sciences for Health, School of Chemistry, University of Birmingham, UK
[3]School of Computer Science, University of Birmingham, UK
[4]Institute of Clinical Sciences, University of Birmingham, UK
[5]Institute of Microbiology and Infection, School of Biosciences, University of Birmingham, UK

Corresponding Authors:

Davor Pavlovic (d.pavlovic@bham.ac.uk
Kashif Rajpoot (k.m.rajpoot@bham.ac.uk)

Email Addresses of Co-authors:

Christopher O'Shea (CXO531@bham.ac.uk)
Andrew P Holmes (A.P.Holmes@bham.ac.uk)
Ting Y Yu (tingyueyu@gmail.com)
James Winter (J.Winter.1@bham.ac.uk)
Simon P Wells (SXW113@student.bham.ac.uk)
Beth Parker (BAP676@student.bham.ac.uk)
Dannie Fobian (DXF608@student.bham.ac.uk)
Daniel M Johnson (D.M.Johnson.1@bham.ac.uk)
Joao Correia (j.correia@cairn-research.co.uk)
Paulus Kirchhof (P.Kirchhof@bham.ac.uk)
Larissa Fabritz (L.Fabritz@bham.ac.uk)

KEYWORDS:

cardiac optical mapping, software, electrophysiology, arrythmia, fluorescent sensors, action potential, calcium

SUMMARY:

This protocol describes the setup and use of ElectroMap, a MATLAB-based open-source software platform for analysis of cardiac optical mapping data. ElectroMap provides a versatile high-throughput tool for analysis of optical mapping voltage and calcium datasets across a wide range of cardiac experimental models.

ABSTRACT:

Optical mapping is an established technique for high spatio-temporal resolution study of cardiac

electrophysiology in multi-cellular preparations. Here we present, in a step-by-step guide, the use of ElectroMap for analysis, quantification, and mapping of high-resolution voltage and calcium datasets acquired by optical mapping. ElectroMap analysis options cover a wide variety of key electrophysiological parameters, and the graphical user interface allows straightforward modification of pre-processing and parameter definitions, making ElectroMap applicable to a wide range of experimental models. We show how built-in pacing frequency detection and signal segmentation allows high-throughput analysis of entire experimental recordings, acute responses, and single beat-to-beat variability. Additionally, ElectroMap incorporates automated multi-beat averaging to improve signal quality of noisy datasets, and here we demonstrate how this feature can help elucidate electrophysiological changes that might otherwise go undetected when using single beat analysis. Custom modules are included within the software for detailed investigation of conduction, single file analysis, and alternans, as demonstrated here. This software platform can be used to enable and accelerate the processing, analysis, and mapping of complex cardiac electrophysiology.

INTRODUCTION:

Optical mapping utilizes fluorescent reporters of voltage and/or calcium concentration to interrogate cardiac electrophysiology (EP) and calcium handling in multicellular preparations, with greater spatial resolution than achievable with traditional techniques[1–3]. Therefore, optical mapping has emerged as an important and ever increasingly utilized technique, providing key insights into physiological and pathophysiological electrical behavior in the heart[3–8]. Effective processing and analysis of data obtained from optical mapping experiments is complicated by several factors. The high spatiotemporal resolution nature of optical mapping datasets results in raw videos files composed of thousands of image frames, each made up of a number of individual pixels, giving rise to large data files that necessitate high-throughput and automated processing[9]. Small pixel sizes, poor and uneven dye loading and small fractional changes in fluorescence result in optical signals with low signal to noise ratio (SNR), requiring pre-processing before effective analysis is achievable[10]. Processing and analysis can be further complicated by the use of optogenetic pacing protocols which utilize light to initiate activation, potentially distorting the recorded signal from the fluorescent sensors[11,12]. Furthermore, once data has been processed, several non-consistent techniques and definitions can be applied to measure parameters of interest, with the most applicable techniques varying depending on experimental setup, model and question[2,10,13]. These limitations prevent further uptake of the technology and hinder truly objective analysis.

To overcome these limitations, several research groups have designed custom processing pipelines tailored towards their experimental model, question and hardware[7,14–16]. Others utilize commercial proprietary software where the underlying algorithms may be difficult to access[4,17]. As a result, there is a clear need for a freely available open-source software platform for processing and analysis of optical mapping data. It is important that this software is open-source, easy to use, flexible to parameter adjustment, applicable to a range of experimental models with distinct EP properties and crucially allows straightforward and tunable quantification of the range of cardiac parameters that can be studied using optical mapping.

We have recently published and released a comprehensive software platform, ElectroMap, for high-throughout, semi-automated processing, analysis and mapping of cardiac optical mapping datasets[13]. Here, we present a video manual for the utilization of ElectroMap and demonstrate how it can be used to process, analyze and map several optical mapping datasets. We focus on the use of ElectroMap to quantify standard EP and calcium handling variables and demonstrate the use of standalone conduction velocity, single file analysis and alternans modules.

PROTOCOL:

1. Optical mapping data collection

1.1. Perform cardiac optical mapping using one of a wide range of experimental models including intact and isolated whole hearts[6,18], isolated atria[14,19], ventricular wedges[20], cardiac slices[21,22], and cellular monolayers[23]. See associated references for experimental designs to collect raw optical mapping data from these preparations. Provided that data obtained can be converted to a tiff stack or saved in a .MAT file, it should be analyzable using ElectroMap. This includes data of varying dimensions (square/rectangular) and resolutions (maximum tested currently 2048 pixels x 2048 pixels).

2. Software installation and start-up

NOTE: Below are detailed the two methods for installing and running ElectroMap – either within MATLAB run from the source (.m) code or as a standalone executable file (.exe for windows). The final software and its functionality are invariant between the two setup options (other than a few differences in directory navigation). Therefore, the main considerations for choosing version to install are access to MATLAB and required toolboxes and whether access to source code is desired. Where possible, it is recommended to use the MATLAB version for faster start up times, shorter processing times, and easier error reporting.

2.1. Setup 1: Running electromap within MATLAB

2.1.1. Install MATLAB. ElectroMap was designed in MATLAB 2017a, however, software has been tested for use in all subsequent releases of MATLAB (up to 2018b at time of writing). The following toolboxes are required: Image Processing, Signal Processing, Statistics and Machine Learning, and Curve Fitting.

2.1.2. Download/clone **all** files from the latest 'source code' release of ElectroMap from the GitHub repository (https://github.com/CXO531/ElectroMap). Unzip the downloaded contents to a desired location.

2.1.3. Open MATLAB and navigate to the folder location hosting the ElectroMap source code. Then, open the file **ElectroMap.m** and press run in the editor, or alternatively type **ElectroMap** in the command window and press **RETURN**. This will start the ElectroMap user interface, **Figure 1A**.

2.2. Setup 2: Standalone .exe file

2.2.1. Download the installer file: https://drive.google.com/open?id=1nJyI07w9WIt5zWcit0aEyIbtg31tANxI.

2.2.2. Follow the instructions in the installer, which will download required the MATLAB runtime from the web alongside ElectroMap software.

2.2.3. Run **ElectroMap.exe**.

NOTE: Start up time for the standalone version can be several minutes.

3. Image loading and pre-processing

3.1. Press **Select Folder** and navigate to the location of the data file(s) to be analyzed. This will populate the left-hand listbox with all files within that directory that are of the correct file type (.tif or .MAT). .MAT files must only contain the image stack variable.

NOTE: Only folders and not individual files will appear as you navigate through the directory selector.

3.2. Select file to be loaded from within the interface and press **Load Images**.

3.2.1. Once loaded, the first frame will appear, and the red outline will indicate automatic thresholding of the image. If needed, reload previously used ROIs by selecting **Save/Load ROI**. In this case, skip step 3.3.

3.2.2. As default, thresholding is based on the pixel intensities in the first frame. If desired, modify this to a threshold based to the signal time course amplitude by changing the option in the **Image for threshold** dropdown menu. Please note that once the thresholding is selected, it is then applied for the whole image stack.

3.3. If desired, change the threshold option to **manual**, which will activate the slider to manually adjust the image threshold. Additionally, crop images (**Crop Image**) and/or draw a custom region of interest (**Custom ROI**) for analysis by selecting the appropriate tick box(es) below threshold options. Note that advanced options for region of interest selection such as number of areas are available from **ROI Selection** from the top menu.

3.4. Once an appropriate threshold has been applied, press **Process Images** to apply processing. Settings for processing are detailed below (step 3.4.1-3.4.5). At this point, ensure that that the correct camera settings have been entered. These are **Pixel Size** in µm (IMPORTANT: this is the image pixel size, and not the size of the pixels that make up the chip or equivalent hardware in the imaging device) and **Framerate** in kHz.

3.4.1. For signal inversion, tick the **Invert Data** checkbox to enable. If reported fluorescent signal is inversely proportional to parameter of interest (as with commonly used potentiometric dyes) the signal can be inverted.

3.4.2. For spatial filtering, select **Gaussian** or **Average** from the kernel menu. The size of the spatially averaged area is controlled by the **Size** input adjacent to the **Kernel** dropdown menu (i.e. 3 results in 3 pixel x 3 pixel filter kernel). When applying a Gaussian filter, the standard deviation can also be set from the **Sigma** input.

3.4.3. For baseline correction, select Top-hat[24] or polynomial (4^{th} or 11^{th} degree) correction[25] from the **Baseline** menu. Correction can be applied to each pixel individually (long processing time) or as an average of the entire image (quicker but assumes homogenous baseline alterations). Top-hat correction can also be modified by setting the **Top-Hat Length** in milliseconds, adjacent to the baseline selection dropdown menu. The length of the Top-Hat kernel should be greater than the timescale of the individual action potentials/calcium transients.

3.4.4. For temporal filtering, select Savitzky-Goaly or infinite impulse (IIR) filtering from the **Filtering** menu.

NOTE: Other than for the tissue averaged signal that appears in the bottom left, temporal filtering is applied to each pixel individually at time of parameter quantification from ensemble averaged image ranges. This has been implemented to reduce processing time by filtering small sections of data when required rather than entire files.

3.4.5. For frame removal, note that if the **Remove Frames** option is selected, large peaks with amplitude greater than the signal of interest can be removed from the image set. This may be useful in optically paced datasets such as optogenetic pacing where depolarization is initiated by optical activation of opsins such as channelrhodopsin 2[11,12].

NOTE: As frame removal will potentially introduce unphysiological step changes into the image signals, temporal filtering may introduce artifacts to the data and so is not recommended here.

3.5. Note that signal will be segmented once **Process Images** has been selected according to the options under **Segmentation options**, however this can quickly be changed without reprocessing the entire dataset (see section 4).

4. Data segmentation and ensemble averaging

NOTE: Once the file has been processed, peaks in the tissue averaged signal (bottom right trace, **Figure 1A**) will have been detected and labelled by red circles. Only peaks above a set threshold (blue line on trace that is set by **Peak Threshold**) are counted. Additionally, peaks are only counted if they are sufficiently delayed compared to the previous peaks, set by the **Min Peak Distance** input. Signal is then segmented based on the detected peaks. First, the effective cycle

length (CL) of each peak is calculated by measuring the time between it and the next peak. If a number of peaks (set by **Min Number of Peaks** input) have similar CLs (threshold for which is set by **Minimum Boundary** input) then they are grouped and the average CL for those peaks calculated.

4.1. For further segmentation of the data, press **Segment Signal**. Sub-segmentation options are: **None** – all peaks with same CL grouped together; **All** – Segments of n_{peaks} within the constant CL times (n_{peaks} is set by the **Segment size** input) are identified; **Last** – Final n_{peaks} before a CL change are identified and grouped, and all others are not analyzed; and **Single Beat** – This is equivalent to applying the **All** segmentation with $n_{peaks} = 1$, and so no grouping or ensemble averaging (see 4.5) are applied. This can be applied by selecting the **Single Beat** button.

4.1.1. Apply custom segmentation of the signal by zooming in on a time of interest and selecting **Segment Signal**. This will add an additional option entitled **Zoomed Section** to the section list box, corresponding to the time points selected.

4.2. The results of the segmentation will appear in the list-box adjacent to the tissue averaged signal, and will show section number and the estimated CL. All segmented time sections are denoted by different colors. Select a segment from the list-box to highlight that section in red. This will also automatically trigger analyses of this section, as if the **Produce Maps** button was selected (see section 5).

4.3. Analyses of grouped peaks will be performed on the 'ensemble averaged' data. This involves averaging the peaks in a segment together, with the reference times being the peaks identified in step 4.2. Update the time window to average by modifying the **before** and **after** inputs and pressing **Segment Signal**.

5. Action potential/calcium transient duration and conduction velocity analysis

5.1. Once images have been processed, the **Produce Maps** button will become active. Press **Produce Maps** to apply action potential duration (APD), activation time, conduction velocity and SNR analysis. By default, the analysis will be applied to the first signal segment. Select other segments from the list-box will apply analysis to chosen segment.

NOTE: Results of analysis are displayed in results table, including mean, standard deviation, standard error, variance and 5th to 95th percentile analysis. Duration maps are termed 'APD' maps however, calcium signals processed using the same settings will measure calcium transient duration.

5.2. Select **Get Pixel Info** to see a detailed display of the signal from any pixel within the image, and **Compare Pixels** to simultaneously plot signals from up to 6 locations.

5.2.1. Use the **Signal Processing** panel to adjust settings for duration analysis. These are: **Duration** – Time of percentage repolarisation/decay to measure from peak; **'APD' Baseline** –

Time period of signal that is defined as reference baseline for amplitude measurements; and **'APD' Start time** – Start time for duration measurements. These are the same options for deciding the activation time for isochronal maps (discussed below) and are termed: Start (d^2F/dt^2_{max}), Upstroke (dF/dt_{max}), Depolarisation midpoint (time of 50% amplitude), Peak (time of maximum amplitude). These definitions applied to mouse and guinea pig action potentials are shown in **Figure 2A**.

NOTE: Changing any of these options will automatically update the duration map and the results table. Map scale and outlier removal options are also available.

5.3. Conduction velocity is also measured automatically within the main software interface. This is achieved using the multi-vector method of Bayly et al[26] from the isochronal map defined by the chosen activation measure (discussed in step 5.4). Press **Activation Points** to render a 3D representation of the activation map.

5.4. The multi-vector conduction velocity measurement method spatially segments the isochronal map into regions of *n* x *n* pixels. Set the value of *n* using the **Local Window Size** input, and set the range of activation times to apply analysis to using the **Fitting activation times** inputs.

NOTE: For each local region, a polynomial surface, *f*, is fitted that best describes the relationship between activation time and spatial position, (*x*,*y*). The gradient vector, CV_{local}, of this surface is then calculated as:

$$CV_{local} = \nabla f(x, y) \quad (1)$$

where ∇ denotes the two-dimensional cartesian spatial differential operator[26].

5.5. For each pixel in the isochronal map, a local vector representing speed and direction of conduction is calculated. Select **Isochronal Map with vectors** from the display dropdown menu to view this analysis.

5.6. SNR is calculated as the ratio of the maximum amplitude compared to the standard deviation of the signal at baseline. This analysis is performed post all processing steps. Press **SNR calculation** in the top menu to edit settings for the period of the signal defined as baseline.

6. Conduction analysis module

6.1. Press **Conduction** to accesses more detailed analysis of conduction velocity. This opens a separate module where conduction can be quantified using the Bayly multi-vector method as in the main interface, single vector methods, and as an activation curve.

6.2. Press **Single Vector** to analyze conduction using the single vector method, where CV is calculated from the delay in activation time between two points. This can be done using **Automatic** or **Manual** methods, selectable below the **Single Vector** button.

6.2.1. For automatic single vector method, select a distance and start point from which to measure conduction. The software will then perform a 360-degree sweep from the selected point, measuring the time delay and calculating the associated conduction velocity along all directions in 1-degree increments. The results of this analysis are displayed in the graph adjacent to the map, and the direction of slowest conduction is shown in red.

6.2.2. For manual single vector method, choose both a start and end point from the isochronal map to calculate conduction velocity. To select a new start point, press **Clear Start Point**.

6.3. Press **Local Vector** to apply the multi vector method, with the settings matching those from the main interface. Within the conduction module, the distribution of conduction speeds, as well as the angular distribution of calculated vectors and angular dependence of conduction speed can be displayed.

6.4. Press activation curve to plot the percentage of tissue activated as a function of time. Time to 100% activation is automatically displayed, while custom values for minimum (blue) and maximum (red) activation percentages between which to measure can also be selected.

7. Additional analyses and modules

7.1.1. Aside from automatically performed duration and conduction velocity analyses, several other parameters can be quantified using ElectroMap. These analyses are selectable from the dropdown menu above the display map. Select one of these options to perform the analysis, and the results will appear in the 4th row of the results table: 1) **Diastolic Interval** – Time from 90% repolarization to activation time of the next action potential; 2) **Dominant Frequency** – Frequency spectrum of each pixel is calculated using the fast Fourier Transform, and the frequency with the most power is defined as the dominant frequency. Advanced range and window settings for dominant frequency analysis are available by selecting **Frequency Mapping**; 3) **Time to peak** – The rise time between two user selected percentages (default 10 to 90%) of the depolarization phase of the action potential or the release of calcium. Percentage values can be changed by selecting **TTP Settings**; and 4) **Relaxation constant** (**τ**) – Relaxation constant is calculated by fitting a mono-exponential decay of the form of the form:

$$F(t) = F_0 e^{-t/\tau} + C \quad (2)$$

where the fluorescence level at time *t* depends on the peak fluorescence, F_0, and the subsequent decay (*C* is a constant)[27]. The value between which to fit equation 2 are selectable within the main ElectroMap user interfaces, as well as a goodness of fit exclusion criteria based on the r^2 value.

7.2. Press **Single File Analysis** to open a dedicated module for high-throughput duration and conduction analysis of each identified segment in a file. Analysis can be performed on either the whole image (duration, conduction and activation time) or on selected regions or points of

interest (currently duration only). Results are outputted to a .csv file.

NOTE: For APD values from the whole image, the first column in the .csv file is the mean, while the second column is the standard deviation.

7.3. Press **Alternans** to initiate a standalone module for dedicated analysis and mapping of beat-to-beat variability. See O'Shea et al. 2019[13] for details on alternans processing and analysis options. Specifically, this module is designed to identify two period oscillations, known as alternans. Both duration and amplitude alternans are calculated and outputted.

NOTE: Duration alternans are measured by comparing the duration measurement from one peak to the next; i.e. if peak one and two and APD_1 and APD_2 respectively, then the duration alternan (ΔAPD) is calculated as

$$\Delta APD = |APD_1 - APD_2| \quad (3)$$

The duration measurement is performed using the settings in the main interface. Meanwhile, amplitude alternans can be quantified and mapped across multi-cellular preparations as absolute change (defined as a percentage where 0% = same amplitude between one beat and the next). Furthermore, the effects of phenomena such as calcium load can be further investigated by measuring and comparing **Load** and **Release** alternans, as has been previously reported[28]. If *L* is defined as the peak amplitude of the large beats (i.e. where the amplitude is greater than the previous beat), *S* the amplitude of the small beats, and *D* the diastolic load of the small beats, the release alternans ($ALT_{release}$) are defined as:

$$ALT_{release} = 1 - (S/L) \quad (4)$$

Conversely, load alternans (ALT_{load}) are defined as:

$$ALT_{load} = D/L \quad (5)$$

Alternans measurements can be made across the whole tissue, and the results of the analysis are displayed in the bottom right of the module. When first using the module, the analysis is performed across the entire experimental file, and the results displayed are an average beat-beat difference across the whole file. However, analysis can be restricted to specific times in the file by de-selecting **Hold Zoom**, zooming in on a specific time period, and selecting **Analyse Zoomed Section**. This will update the results panel to show analysis from the selected time period.

7.3.1. Select play to show a beat-to-beat video of the alternans analysis. Additionally, select **Create Mean Map** to export a map of the alternans behavior averaged from the selecting time points, which are set in the pop-up menu when using this feature.

7.4. Press **Phase Map** to initiate the phase mapping module. A Hilbert transform is performed to calculate the instantaneous phase (between -π and +π) of the signals at each timepoint. Press

play or drag slider to visualize phase behavior over time and click on a pixel to render a phase diagram.

8. Exporting data

8.1. Data is exported from ElectroMap in a variety of forms. Press **Export Values** to save the values of the currently displayed map in the main used interface. Measured values can be saved as either a map (preserving pixel locations) or condensed into a single list, and can be saved as .csv,.txt or .MAT files.

8.2. Press **Export Map** to bring up a pop-up containing the currently displayed map, which can then be saved in a variety of image formats. Display options for the map are controlled by selecting **Map Settings** but can also be edited once **Export Map** has been selected. For example, a color bar can be added by selecting this icon from the top menu, and the scale can be set by selecting **Edit** > **Colormap**.

8.3. Press **Activation Video** to render an animation of the activation sequence, which can be saved as an animated .gif file.

8.4. Press **Segment Video** to save a .avi video file of the currently displayed parameter of each identified segment.

REPRESENTATIVE RESULTS:

All work performed as part of this study was undertaken in accordance with ethical guidelines set out by the UK Animals (Scientific Procedures) Act 1986 and Directive 2010/63/EU of the European Parliament on the protection of animals used for scientific purposes. Experiments were approved by the home office (mouse: PPL 30/2967 and PFDAAF77F, guinea pig: PPL PF75E5F7F) and the institutional review boards at University of Birmingham (mouse) and King's College London (guinea pig). Detailed methods for collection of the raw data that has been analyzed here can be found in our previous publications[5,6,14,19].

The main interface from which ElectroMap is controlled is shown in **Figure 1A**. The necessary steps to analyze a dataset are controlled primarily by the **Load Images**, **Process Images**, and **Produce Maps** buttons, and are shown highlighted in green, blue, and red, respectively in **Figure 1A**. **Figure 1B–D** shows the operations that occur on selection of each of these buttons. **Load Images** applies the image thresholding options as selected by the user (**Figure 1B**), while **Process Images** (**Figure 1C**) applies filtering and baseline correction. Finally, **Produce Maps** will first average data according to the time window and segmentation settings (unless single beat segmentation is chosen) and then perform analyses described above.

A key aspect of ElectroMap is its flexibility with respect to camera type and experimental model. This is crucial for the utility of an optical mapping software due to the distinct cardiac EP and anatomical characteristics that exist between widely used models. **Figure 2A** for example shows

the action potential morphology of the murine atria when compared to the guinea pig ventricle, recorded using voltage sensitive dyes as previously reported[6,14]. Despite the distinct shape of the action potential, and the use of two separate optical mapping cameras with different framerates and pixel sizes, ElectroMap can be utilized to successfully analyze both datasets. However, this requires modification of some parameters within the user interface (**Figure 2B**). Note that the prolonged guinea pig action potential necessitates a larger time window. Additionally, to prevent top-hat baseline correction unphysiologically modifying the optically recorded signals, its time length must be increased so that it is greater than the time course of the action potential.

ElectroMap offers a multitude of processing options to help improve the SNR of optically recorded signals which may be required to effectively recover EP parameters. An example is automated ensemble averaging of peaks following data segmentation. **Figure 3A–C** demonstrates how the application of ensemble averaging, in lieu of other methods, can improve SNR from isolated murine left atria (*n* = 13). This reduces measurement heterogeneity and likelihood of analysis failure (**Figure 3D**). For example, a change of pacing frequency from 3 Hz to 10 Hz did not alter APD_{50}, when no ensemble averaging is undertaken, yet an expected[29] decrease in APD_{50} at 10 Hz pacing was observed when measured from ensemble averaged data (**Figure 3E**).

Figure 4 demonstrates the efficacy and utility of automated pacing frequency detection and segmentation offered by ElectroMap. Here, mouse left atria (n = 5) were paced at a 120 ms cycle length and cycle length was incrementally shortened by 10 ms until it reached 50 ms. ElectroMap automatically identified the pacing cycle length and grouped tissue averaged peaks accordingly (**Figure 4A**). This was achieved with high accuracy in all datasets (**Figure 4B**). Automated segmentation of the data allowed straightforward and high throughput analysis of the slowing of conduction velocity with increased pacing frequency/shortened cycle length (**Figure 4C,D**). Concurrently, APD_{50} (**Figure 4E**) and diastolic interval (**Figure 4F**) shortened. Amplitude of the optically measured peaks decreased, while time to peak increased **(Figure 4G,H**). These are again the expected restitution responses in cardiac tissue[29,30] and use of ElectroMap can help therefore elucidate changes in response to pacing frequency in presence of pharmacological agents, genetic modification, or disease states.

An important consideration in the use of a software such as ElectroMap is the presence of artifacts in the underlying data. **Figure 5**, for example demonstrates that motion artifacts (the distortion of the optically recorded signal by tissue movement) can preclude accurate measurements of activation and especially repolarization within ElectroMap. See Discussion for further considerations.

FIGURE AND TABLE LEGENDS:

Figure 1: ElectroMap main processing steps. (**A**) Graphical user interface of ElectroMap, with the **Load Images** (green), **Process Images** (blue), and **Produce Maps** (red) buttons highlighted. (**B**) Image thresholding options that can be applied on selecting **Load Images**. (**C**) Signal processing options available to the user include spatial and temporal filtering and baseline correction and

can be applied to the image stack by pressing **Process Images**. (**D**) Ensemble averaging and parameter quantification (shown APD measurement) that is activated by selecting **Produce Maps**. Figure adapted from O'Shea et al., 2019[13].

Figure 2: Analysis of mouse and guinea pig data using ElectroMap. (**A**) Optically recorded action potential from mouse atria and guinea pig ventricles, along with both the first (df/dt) and second (d^2f/dt^2) derivate of these signals. The various definitions for activation and repolarization times employable within ElectroMap are highlighted. (**B**) Screenshots of Image and signal processing settings utilized in ElectroMaps interface. Red boxes highlight settings that required modification between analyses of mouse and guinea pig data. Figure adapted from O'Shea et al., 2019[13].

Figure 3: Ensemble averaging to resolve APD changes. (**A**) APD_{50} map and example single pixel signal from single beat optical action potentials. (**B**) APD_{50} map and example single pixel signal from optical action potentials generated by ensemble averaging of 10 successive beats (peak method). (**C**) SNR of single beat compared to 10 beat averaged signals. (**D**) APD_{50} heterogeneity (i) and number of measurement failures (ii) as a function of SNR for single beat and 10 beat averaged APD_{50} maps. (**E**) APD_{50} at 3 and 10 Hz pacing frequency, as measured from single beat and 10 beat maps. (Data shown as mean ± standard error, n = 13 left atria, ****$p < 0.001$ by student's paired t-test).

Figure 4: Use of ElectroMap to study pacing frequency responses in cardiac tissue. (**A**) Example ElectroMap screenshot of pacing frequency recognition and segmentation. (**B**) Comparison of known and ElectroMap measured pacing cycle lengths. (**C**) Activation maps at 120 ms and 60 ms pacing cycle lengths. (**D–H**) Grouped data of conduction velocity (**D**), APD_{50} (**E**), diastolic interval (**F**), amplitude (**G**), and time to peak (**H**) as a function of pacing cycle length decreasing from 120 ms to 60 ms in 10 ms increments. (Data shown as mean ± standard error, n = 5 left atria)

Figure 5. Effect of motion artifacts. (**A**) APD_{50} map. (**B**) Activation map. (**C**) Example signals from locations marked (crosses) on APD and activation maps. In the area of the tissue marked with the red cross, contraction has not been successfully uncoupled, distorting the measured optical signal.

DISCUSSION:

Here, we present a step-by-step guide for the utilization of open-source software ElectroMap for flexible and multi variable analysis of cardiac optical mapping datasets. For successful use of ElectroMap, imaging data is required to be in .tif or .MAT formats. ElectroMap incorporates several modifiable user settings. As demonstrated in **Figure 2A**, this is necessary due to the wide heterogeneity that exists between experimental models and imaging hardware. This means however that default settings within the software will not always be optimal, so a critical step in using the software is for the user to tune settings for their particular experimental setup. These include camera settings and timescales, as shown in **Figure 2B**. Once optimal settings have been found, these can be saved and reloaded at later times by selecting **Configuration File**.

Incorporation of automated CL measurement and signal segmentation are key advantages of the software. These features allow analysis of acute responses in experimental recordings and widen analysis from focusing on isolated single beats. Once desired segmentation has been achieved, the **Single File Analysis** module allows automated analysis of each individual segment (including single beats), realizing high-throughput analysis of multiple variables across the recording outputted in a single .csv file. In conjunction, ensemble averaging of grouped peaks is an effective method to improve quality of noisy signals that is automatically performed in ElectroMap. However, ensemble averaging is not ubiquitously beneficial, for example in studies of beat-to-beat variability. Therefore, ElectroMap integrates single beat segmentation to avoid ensemble averaging, alternative processing options to improve SNR (spatial and temporal filtering) and includes the **Alternans** analysis module to further investigate and map beat-to-beat variability.

Optical Mapping datasets often exhibit artifacts such as baseline drift and motion artifacts. Equally, the signals generated can be low quality due to small pixel sizes, short exposure times and low fractional fluorescent changes[2]. These factors prevent effective and accurate analysis of the underlying EP behavior. As outlined, ElectroMap has several processing strategies to overcome these issues. However, application of these algorithms to fundamentally poor quality/distorted data will still prevent effective analysis. SNR is therefore one of the parameters that is measured and displayed in ElectroMap. Equally, the user can select and compare the signals from specific regions from the sample using the **Pixel Info** and **Compare** modules, allowing identification of phenomena such as motion artifacts shown in **Figure 5**, and appropriate exclusion of data.

At present, ElectroMap does not support removal of motion artifacts from raw data in the same manner as baseline correction. Therefore, a possible future development of the software is inclusion of motion artefact removal by computational methods as has been reported[31,32]. Furthermore, ElectroMap is currently limited to study of one optical signal. However, for ratiometric dyes and simultaneous use of voltage and calcium dyes[27], concurrent processing of two wavelength channels is required. The integration of dual signal analysis is therefore an important future addition to the software. Extension of analysis options applicable to arrhythmic datasets, such as phase singularity tracking, would equally broaden the scope of the software[33,34]. Finally, several of the analysis options described can also be useful in analysis of the electrode mapping data. Indeed, ElectroMap has been used to analyze electrode mapping data despite the contrasting electrogram waveform[20,35], and further optimization will expand its use for this modality.

ACKNOWLEDGMENTS:

This work was funded by the EPSRC studentship (Sci-Phy-4-Health Centre for Doctoral Training L016346) to D.P., K.R. and L.F., Wellcome Trust Seed Award Grant (109604/Z/15/Z) to D.P., British Heart Foundation Grants (PG/17/55/33087, RG/17/15/33106) to D.P., European Union (grant agreement No 633196 [CATCH ME] to P.K. and L.F.), British Heart Foundation (FS/13/43/30324 to P.K. and L.F.; PG/17/30/32961 to P.K. and A.H.), and Leducq Foundation to P.K.. J.W. is supported by the British Heart Foundation (FS/16/35/31952).

DISCLOSURES:

P.K. receives research support from several drug and device companies active in atrial fibrillation and has received honoraria from several such companies. L.F. has received institutional research grants EU, BHF, MRC, DFG and Gilead. P.K. and L.F. are listed as inventors on two patents held by University of Birmingham (Atrial Fibrillation Therapy WO 2015140571, Markers for Atrial Fibrillation WO 2016012783).

All other authors declare no potential conflict of interest.

REFERENCES:

1. Efimov, I. R., Nikolski, V. P., Salama, G. Optical Imaging of the Heart. *Circulation Research.* **94,** 21–33 (2004).
2. Herron, T. J., Lee, P., Jalife, J. Optical imaging of voltage and calcium in cardiac cells & tissues. *Circulation Research.* **110,** 609–623 (2012).
3. Boukens, B. J., Efimov, I. R. A century of optocardiography. *IEEE Reviews in Biomedical Engineering.* **7,** 115–125 (2014).
4. Myles, R. C., Wang, L., Kang, C., Bers, D. M., Ripplinger, C. M. Local β-adrenergic stimulation overcomes source-sink mismatch to generate focal arrhythmia. *Circulation Research.* **110,** 1454–1464 (2012).
5. Syeda, F. et al. PITX2 Modulates Atrial Membrane Potential and the Antiarrhythmic Effects of Sodium-Channel Blockers. *Journal of the American College of Cardiology.* **68,** 1881–1894 (2016).
6. Winter, J. et al. Sympathetic nervous regulation of cardiac alternans in the intact heart. *Frontiers in Physiology.* **9,** 1–12 (2018).
7. Faggioni, M. et al. Suppression of spontaneous ca elevations prevents atrial fibrillation in calsequestrin 2-null hearts. *Circulation: Arrhythmia and Electrophysiology.* **7,** 313–320 (2014).
8. Sato, P. Y. et al. Loss of Plakophilin-2 Expression Leads to Decreased Sodium Current and Slower Conduction Velocity in Cultured Cardiac Myocytes. *Circulation Research.* **105,** 523–526 (2009).
9. Yu, T. Y. et al. Optical mapping design for murine atrial electrophysiology. *Computer Methods in Biomechanics and Biomedical Engineering: Imaging & Visualization.* **5,** 368–378 (2017).
10. Laughner, J. I., Ng, F. S., Sulkin, M. S., Arthur, R. M., Efimov, I. R. Processing and analysis of cardiac optical mapping data obtained with potentiometric dyes. *American Journal of Physiology. Heart and Circulatory Physiology.* **303,** H753-65 (2012).
11. Crocini, C., Ferrantini, C., Pavone, F. S., Sacconi, L. Optogenetics gets to the heart: A guiding light beyond defibrillation. *Progress in Biophysics and Molecular Biology.* **130,** 132–139 (2017).
12. Entcheva, E., Bub, G. All-optical control of cardiac excitation: Combined high-resolution optogenetic actuation and optical mapping. *The Journal of Physiology.* **9,** 2503–2510

(2016).
13. O'Shea, C. et al. ElectroMap: High-throughput open-source software for analysis and mapping of cardiac electrophysiology. *Scientific Reports.* **9,** 1–13 (2019).
14. Yu, T. Y. et al. An automated system using spatial oversampling for optical mapping in murine atria. Development and validation with monophasic and transmembrane action potentials. *Progress in Biophysics and Molecular Biology.* **115,** 340–348 (2014).
15. Jaimes, R. et al. Functional response of the isolated, perfused normoxic heart to pyruvate dehydrogenase activation by dichloroacetate and pyruvate. *Pflugers Archiv.* **468,** 131–142 (2016).
16. Wang, K. et al. Cardiac tissue slices: preparation, handling, and successful optical mapping. *American Journal of Physiology. Heart and Circulatory Physiology.* **308,** H1112-25 (2015).
17. Parrish, D. C. et al. Transient denervation of viable myocardium after myocardial infarction does not alter arrhythmia susceptibility. *American Journal of Physiology. Heart and Circulatory Physiology.* doi:10.1152/ajpheart.00300.2017 (2017).
18. Ihara, K. et al. Electrophysiological Assessment of Murine Atria with High-Resolution Optical Mapping. *Journal of Visualized Experiments.* **132,** e56478 (2018).
19. Holmes, A. P. et al. A Regional Reduction in Ito and IKACh in the Murine Posterior Left Atrial Myocardium Is Associated with Action Potential Prolongation and Increased Ectopic Activity. *Plos One.* **11,** e0154077 (2016).
20. Lang, D. et al. Arrhythmogenic remodeling of β<inf>2</inf> versus β<inf>1</inf> adrenergic signaling in the human failing heart. *Circulation: Arrhythmia and Electrophysiology.* **8,** 409–419 (2015).
21. Kang, C. et al. Human Organotypic Cultured Cardiac Slices: New Platform For High Throughput Preclinical Human Trials. *Scientific Reports.* **6,** 1–13 (2016).
22. Wen, Q. et al. Transverse cardiac slicing and optical imaging for analysis of transmural gradients in membrane potential and Ca2+ transients in murine heart. *The Journal of Physiology.* **596,** 3951–3965 (2018).
23. Houston, C. et al. Characterisation of re-entrant circuit (or rotational activity) in vitro using the HL1-6 myocyte cell line. *Journal of Molecular and Cellular Cardiology.* **119,** 155–164 (2018).
24. Yu, T. Y. et al. Optical mapping design for murine atrial electrophysiology. *Computer Methods in Biomechanics and Biomedical Engineering: Imaging and Visualization* **5,** 368–376 (2017).
25. Laughner, J. I., Ng, F. S., Sulkin, M. S., Arthur, R. M., Efimov, I. R. Processing and analysis of cardiac optical mapping data obtained with potentiometric dyes. *AJP: Heart and Circulatory Physiology.* **303,** H753–H765 (2012).
26. Bayly, P. V et al. Estimation of Conduction Velocity Vector Fields from Epicardial Mapping Data. *IEEE Transactions on Bio-Medical Engineering.* **45,** 563–571 (1998).
27. Jaimes, R. et al. A technical review of optical mapping of intracellular calcium within myocardial tissue. *American Journal of Physiology. Heart and Circulatory Physiology.* **310,** H1388–H1401 (2016).
28. Wang, L. et al. Optical mapping of sarcoplasmic reticulum Ca2+ in the intact heart: Ryanodine receptor refractoriness during alternans and fibrillation. *Circulation Research.* **114,** 1410–1421 (2014).

29. Winter, J., Shattock, M. J. Geometrical considerations in cardiac electrophysiology and arrhythmogenesis. *Europace.* doi:10.1093/europace/euv307 (2016).
30. Mironov, S., Jalife, J., Tolkacheva, E. G. Role of conduction velocity restitution and short-term memory in the development of action potential duration alternans in isolated rabbit hearts. *Circulation.* **118,** 17–25 (2008).
31. Khwaounjoo, P. et al. Image-Based Motion Correction for Optical Mapping of Cardiac Electrical Activity. *Annals of Biomedical Engineering.* **43,** 1235–1246 (2014).
32. Christoph, J., Luther, S. Marker-Free Tracking for Motion Artifact Compensation and Deformation Measurements in Optical Mapping Videos of Contracting Hearts. *Frontiers in Physiology.* **9,** (2018).
33. Umapathy, K. et al. Phase Mapping of Cardiac Fibrillation. *Circulation: Arrhythmia and Electrophysiology.* **3,** 105–114 (2010).
34. Tomii, N. et al. Detection Algorithm of Phase Singularity Using Phase Variance Analysis for Epicardial Optical Mapping Data. *IEEE Transactions on Biomedical Engineering.* **63,** 1795–1803 (2016).
35. Cantwell, C. D. et al. Techniques for automated local activation time annotation. and conduction velocity estimation in cardiac mapping. *Computers in Biology and Medicine* **65,** (2015).

Figure 1

Click here to access/download;Figure;Figure 1.pdf

A

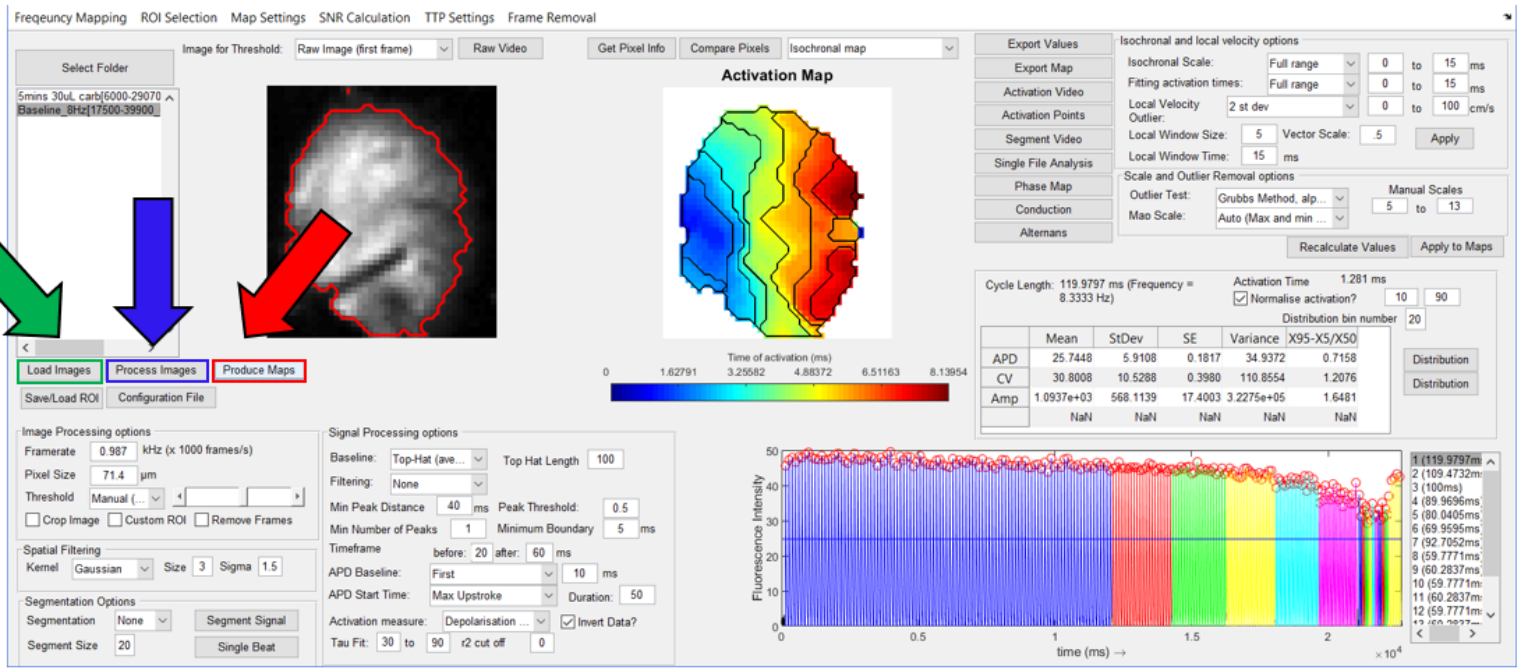

B

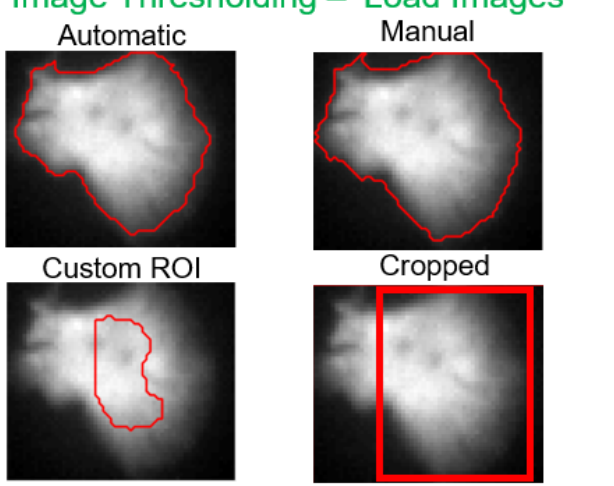

C

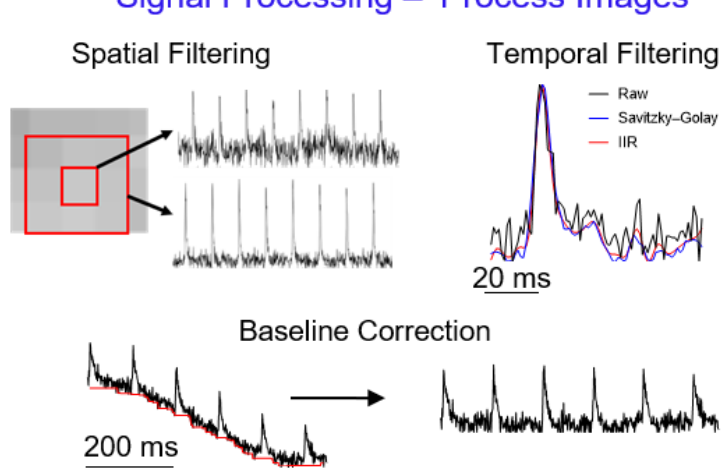

D

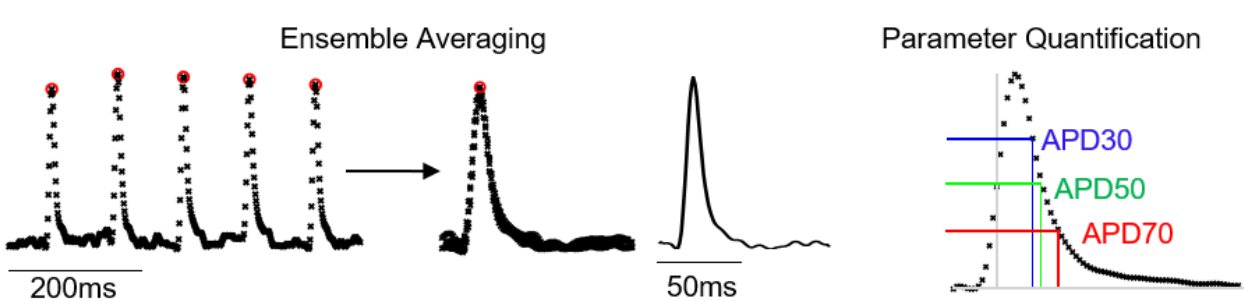

Figure 2

Click here to access/download;Figure;Figure 2.pdf

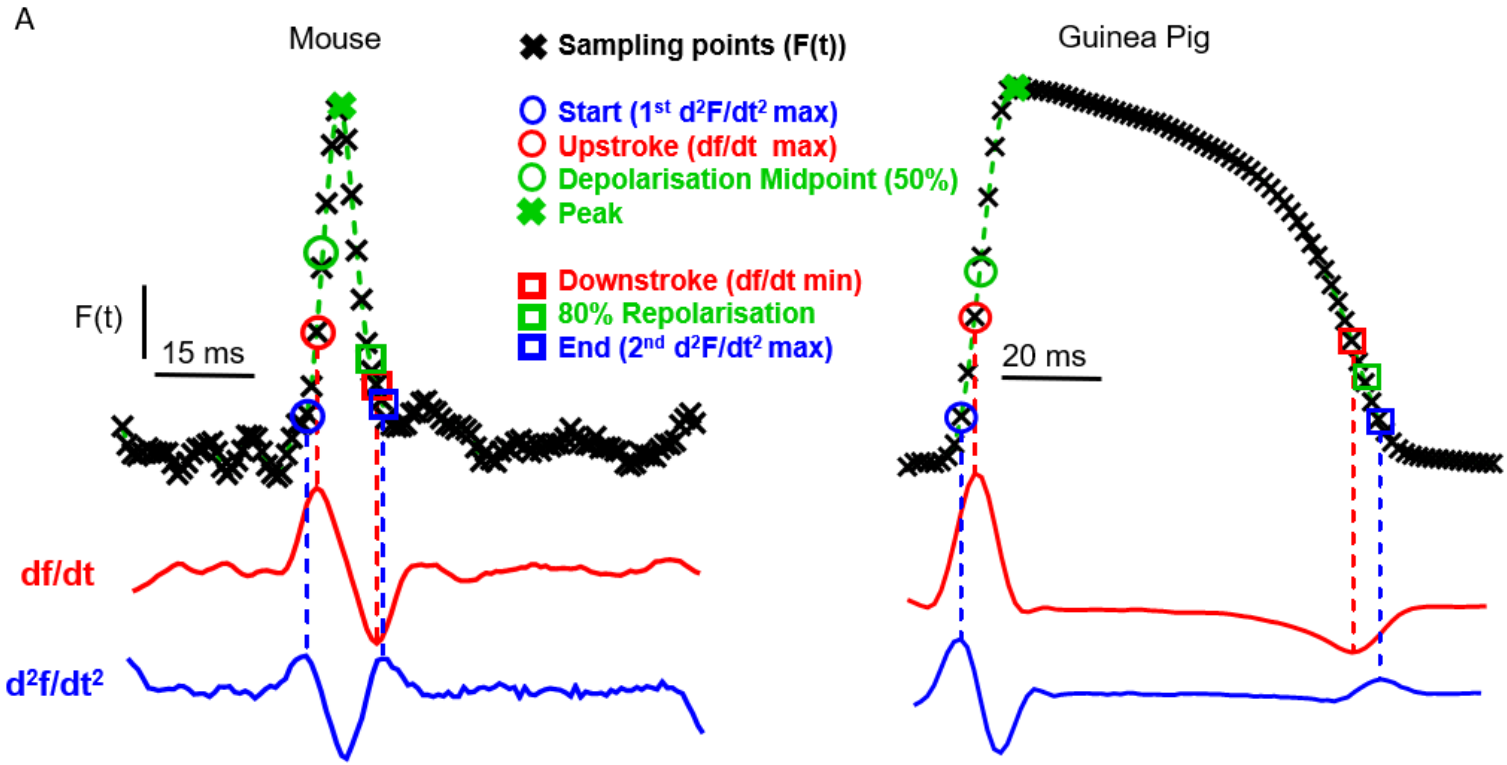

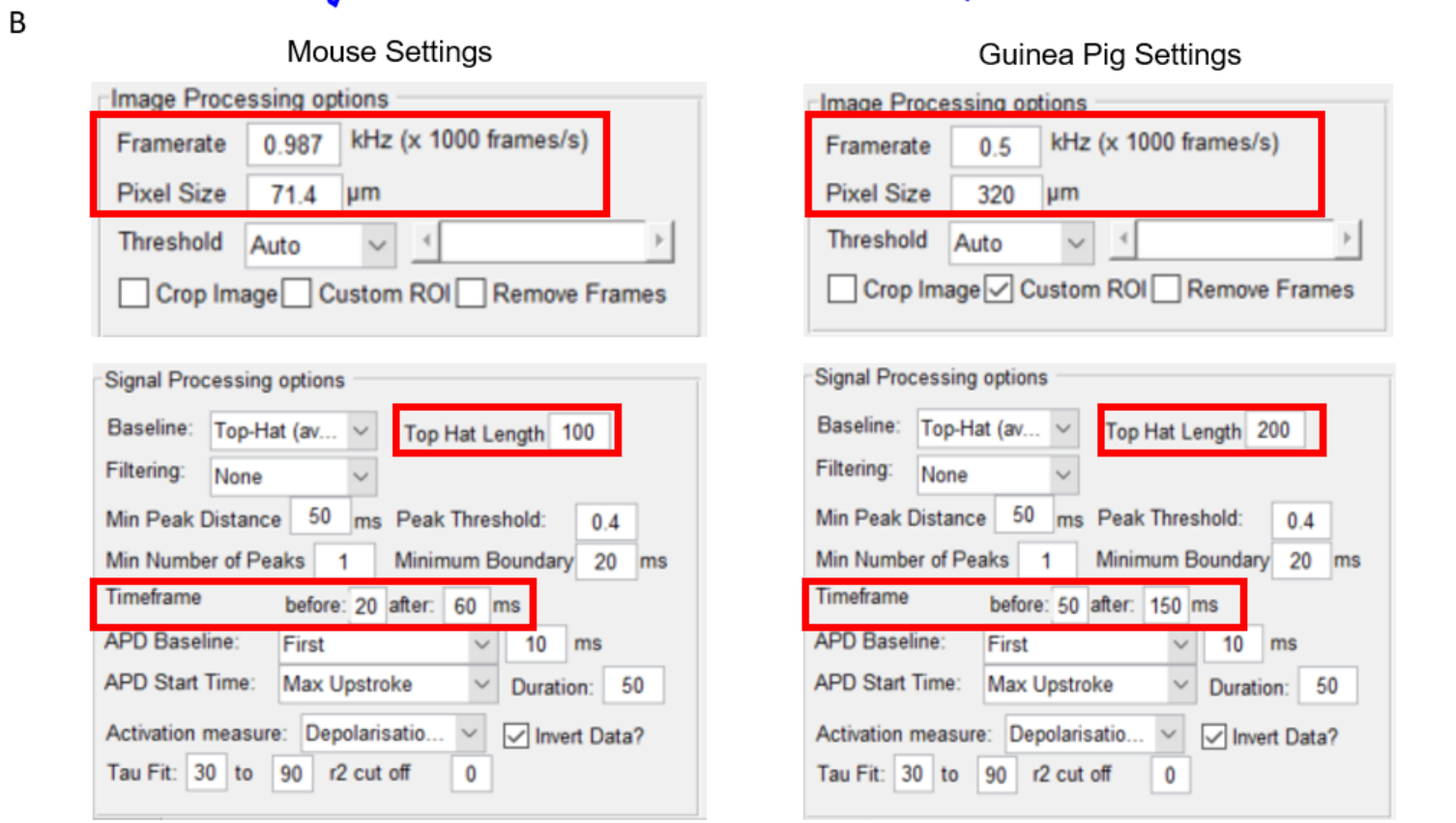

Figure 3

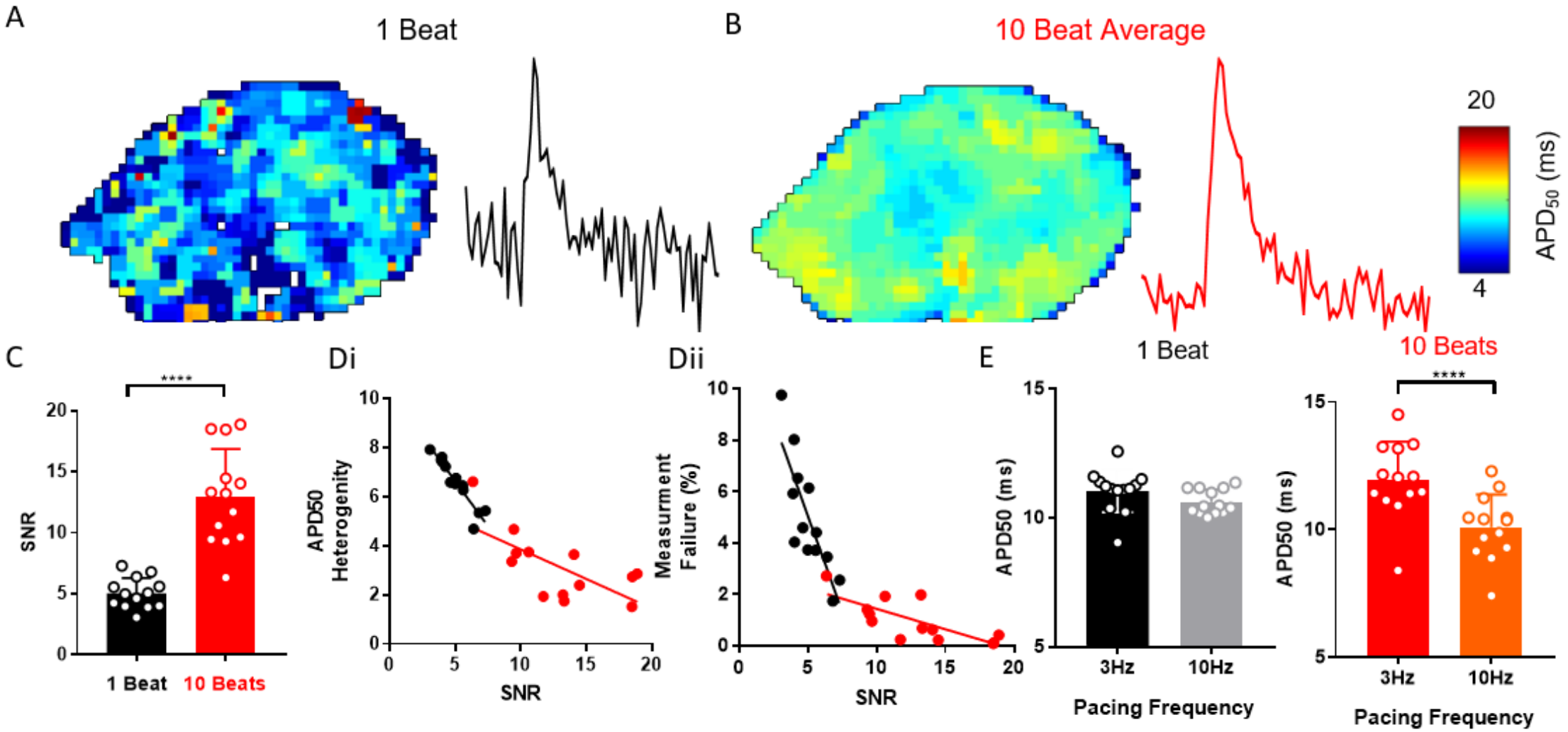

Figure 4

Click here to access/download;Figure;Figure 4.pdf

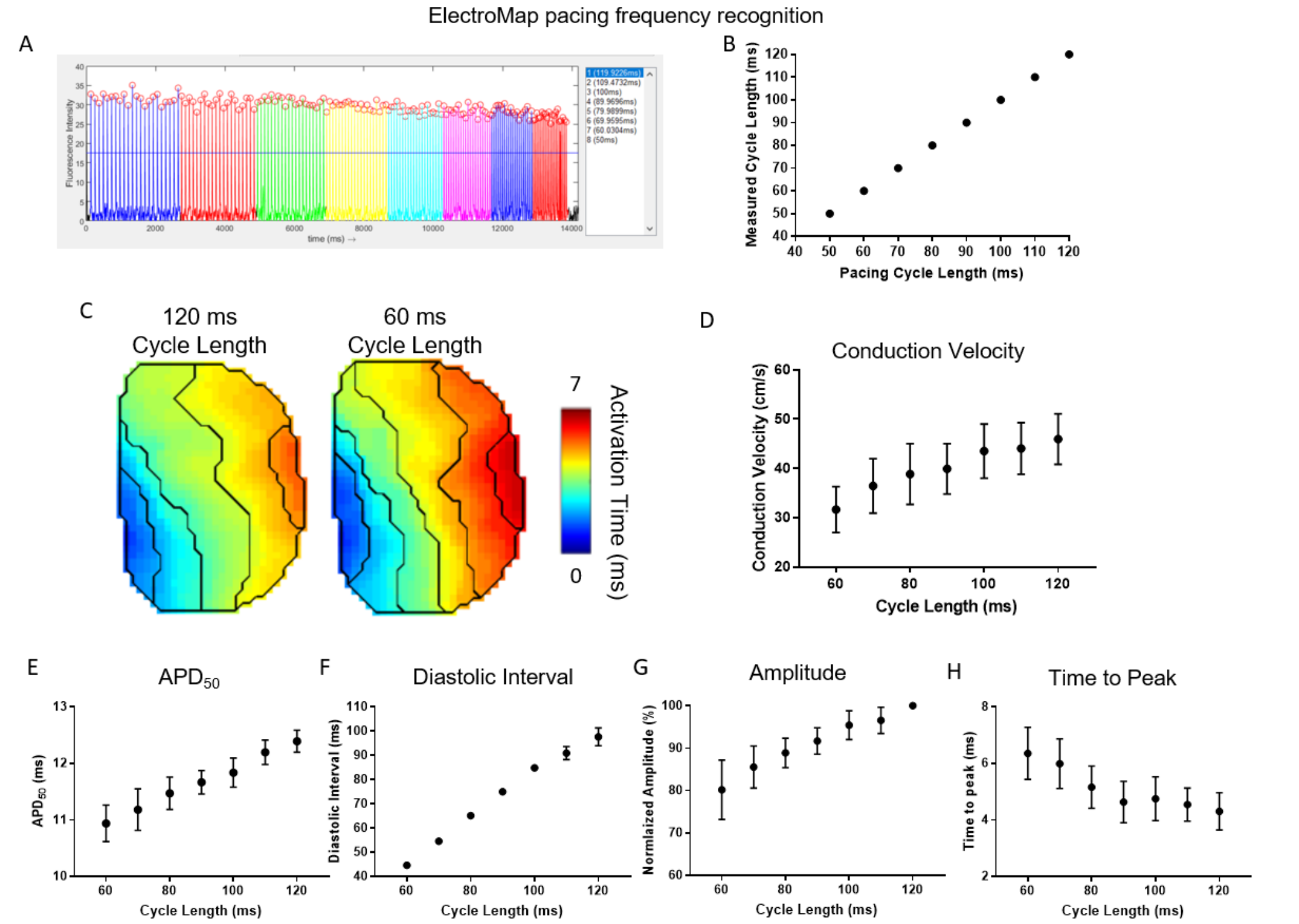

Figure 5

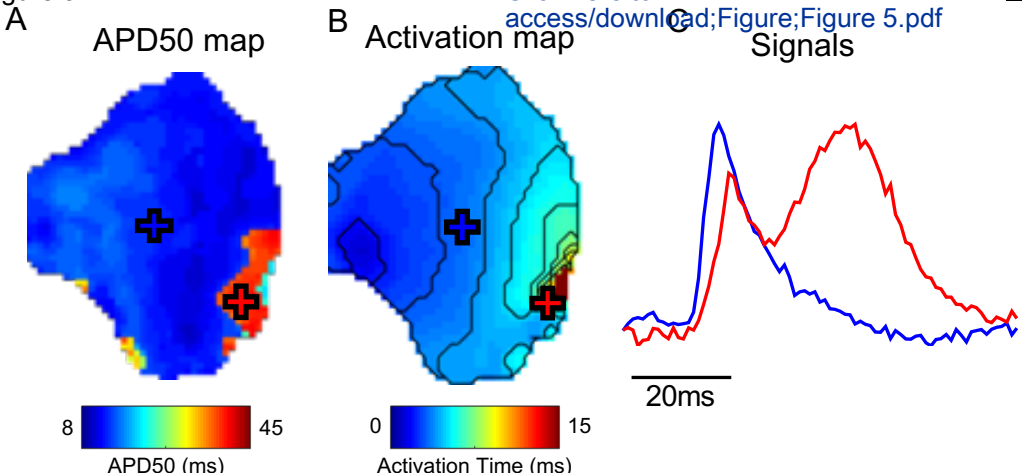

Name of Material/ Equipment	Company	Catalog Number	Comments/Description
MATLAB and Simulink R2018a	Mathworks, Inc, Natick, MA		MATLAB software

jove JOURNAL OF VISUALIZED EXPERIMENTS
1 Alewife Center #200
Cambridge, MA 02140
tel. 617.945.9051
www.jove.com

ARTICLE AND VIDEO LICENSE AGREEMENT - UK

Title of Article:	ElectroMap software for high throughput analysis of cardiac optical mapping datasets
Author(s):	Christopher O'Shea, Andrew P Holmes, Ting Y Yu, James Winter, Simon P Wells, Joao Correia, Paulus Kirchhof, Larissa Fabritz, Kashif Rajpoot, Davor Pavlovic

Item 1: The Author elects to have the Materials be made available (as described at http://www.jove.com/publish) via:

☐ Standard Access ■ Open Access

Item 2: Please select one of the following items:

■ The Author is **NOT** a United States government employee.

☐ The Author is a United States government employee and the Materials were prepared in the course of his or her duties as a United States government employee.

☐ The Author is a United States government employee but the Materials were NOT prepared in the course of his or her duties as a United States government employee.

ARTICLE AND VIDEO LICENSE AGREEMENT

1. **Defined Terms.** As used in this Article and Video License Agreement, the following terms shall have the following meanings: "**Agreement**" means this Article and Video License Agreement; "**Article**" means the article specified on the last page of this Agreement, including any associated materials such as texts, figures, tables, artwork, abstracts, or summaries contained therein; "**Author**" means the author who is a signatory to this Agreement; "**Collective Work**" means a work, such as a periodical issue, anthology or encyclopedia, in which the Materials in their entirety in unmodified form, along with a number of other contributions, constituting separate and independent works in themselves, are assembled into a collective whole; "**CRC License**" means the Creative Commons Attribution 3.0 Agreement (also known as CC-BY), the terms and conditions of which can be found at: http://creativecommons.org/licenses/by/3.0/us/legalcode ; "**Derivative Work**" means a work based upon the Materials or upon the Materials and other pre-existing works, such as a translation, musical arrangement, dramatization, fictionalization, motion picture version, sound recording, art reproduction, abridgment, condensation, or any other form in which the Materials may be recast, transformed, or adapted; "**Institution**" means the institution, listed on the last page of this Agreement, by which the Author was employed at the time of the creation of the Materials; "**JoVE**" means MyJove Corporation, a Massachusetts corporation and the publisher of The Journal of Visualized Experiments; "**Materials**" means the Article and / or the Video; "**Parties**" means the Author and JoVE; "**Video**" means any video(s) made by the Author, alone or in conjunction with any other parties, or by JoVE or its affiliates or agents, individually or in collaboration with the Author or any other parties, incorporating all or any portion of the Article, and in which the Author may or may not appear.

2. **Background.** The Author, who is the author of the Article, in order to ensure the dissemination and protection of the Article, desires to have the JoVE publish the Article and create and transmit videos based on the Article. In furtherance of such goals, the Parties desire to memorialize in this Agreement the respective rights of each Party in and to the Article and the Video.

3. **Grant of Rights in Article.** In consideration of JoVE agreeing to publish the Article, the Author hereby grants to JoVE, subject to **Sections 4 and 7** below, the exclusive,

royalty-free, perpetual (for the full term of copyright in the Article, including any extensions thereto) license (a) to publish, reproduce, distribute, display and store the Article in all forms, formats and media whether now known or hereafter developed (including without limitation in print, digital and electronic form) throughout the world, (b) to translate the Article into other languages, create adaptations, summaries or extracts of the Article or other Derivative Works (including, without limitation, the Video) or Collective Works based on all or any portion of the Article and exercise all of the rights set forth in (a) above in such translations, adaptations, summaries, extracts, Derivative Works or Collective Works and (c) to license others to do any or all of the above. The foregoing rights may be exercised in all media and formats, whether now known or hereafter devised, and include the right to make such modifications as are technically necessary to exercise the rights in other media and formats. If the "Open Access" box has been checked in **Item 1** above, JoVE and the Author hereby grant to the public all such rights in the Article as provided in, but subject to all limitations and requirements set forth in, the CRC License.

4. **Retention of Rights in Article.** Notwithstanding the exclusive license granted to JoVE in **Section 3** above, the Author shall, with respect to the Article, retain the non-exclusive right to use all or part of the Article for the non-commercial purpose of giving lectures, presentations or teaching classes, and to post a copy of the Article on the Institution's website or the Author's personal website, in each case provided that a link to the Article on the JoVE website is provided and notice of JoVE's copyright in the Article is included. All non-copyright intellectual property rights in and to the Article, such as patent rights, shall remain with the Author.

5. **Grant of Rights in Video - Standard Access.** This **Section 5** applies if the "Standard Access" box has been checked in **Item 1** above or if no box has been checked in **Item 1** above. In consideration of JoVE agreeing to produce, display or otherwise assist with the Video, the Author hereby acknowledges and agrees that, subject to **Section 7** below, JoVE is and shall be the sole and exclusive owner of all rights of any nature, including, without limitation, all copyrights, in and to the Video. To the extent that, by law, the Author is deemed, now or at any time in the future, to have any rights of any nature in or to the Video, the Author hereby disclaims all such rights and transfers all such rights to JoVE.

6. **Grant of Rights in Video - Open Access.** This **Section 6** applies only if the "Open Access" box has been checked in **Item 1** above. In consideration of JoVE agreeing to produce, display or otherwise assist with the Video, the Author hereby grants to JoVE, subject to **Section 7** below, the exclusive, royalty-free, perpetual (for the full term of copyright in the Article, including any extensions thereto) license (a) to publish, reproduce, distribute, display and store the Video in all forms, formats and media whether now known or hereafter developed (including without limitation in print, digital and electronic form) throughout the world, (b) to translate the Video into other languages, create adaptations, summaries or extracts of the Video or other Derivative Works or Collective Works based on all or any portion of the Video and exercise all of the rights set forth in (a) above in such translations, adaptations, summaries, extracts, Derivative Works or Collective Works and (c) to license others to do any or all of the above. The foregoing rights may be exercised in all media and formats, whether now known or hereafter devised, and include the right to make such modifications as are technically necessary to exercise the rights in other media and formats.

7. **Government Employees.** If the Author is a United States government employee and the Article was prepared in the course of his or her duties as a United States government employee, as indicated in **Item 2** above, and any of the licenses or grants granted by the Author hereunder exceed the scope of the 17 U.S.C. 403, then the rights granted hereunder shall be limited to the maximum rights permitted under such statute. In such case, all provisions contained herein that are not in conflict with such statute shall remain in full force and effect, and all provisions contained herein that do so conflict shall be deemed to be amended so as to provide to JoVE the maximum rights permissible within such statute.

8. **Protection of the work.** The Author(s) authorize JoVE to take steps in the Author(s) name and on their behalf if JoVE believes some third party could be infringing or might infringe the copyright of either the Author's Article and/or Video.

9. **Likeness, Privacy, Personality.** The Author hereby grants JoVE the right to use the Author's name, voice, likeness, picture, photograph, image, biography and performance in any way, commercial or otherwise, in connection with the Materials and the sale, promotion and distribution thereof. The Author hereby waives any and all rights he or she may have, relating to his or her appearance in the Video or otherwise relating to the Materials, under all applicable privacy, likeness, personality or similar laws.

10. **Author Warranties**. The Author represents and warrants that the Article is original, that it has not been published, that the copyright interest is owned by the Author (or, if more than one author is listed at the beginning of this Agreement, by such authors collectively) and has not been assigned, licensed, or otherwise transferred to any other party. The Author represents and warrants that the author(s) listed at the top of this Agreement are the only authors of the Materials. If more than one author is listed at the top of this Agreement and if any such author has not entered into a separate Article and Video License Agreement with JoVE relating to the Materials, the Author represents and warrants that the Author has been authorized by each of the other such authors to execute this Agreement on his or her behalf and to bind him or her with respect to the terms of this Agreement as if each of them had been a party hereto as an Author. The Author warrants that the use, reproduction, distribution, public or private

performance or display, and/or modification of all or any portion of the Materials does not and will not violate, infringe and/or misappropriate the patent, trademark, intellectual property or other rights of any third party. The Author represents and warrants that it has and will continue to comply with all government, institutional and other regulations, including, without limitation all institutional, laboratory, hospital, ethical, human and animal treatment, privacy, and all other rules, regulations, laws, procedures or guidelines, applicable to the Materials, and that all research involving human and animal subjects has been approved by the Author's relevant institutional review board.

11. **JoVE Discretion.** If the Author requests the assistance of JoVE in producing the Video in the Author's facility, the Author shall ensure that the presence of JoVE employees, agents or independent contractors is in accordance with the relevant regulations of the Author's institution. If more than one author is listed at the beginning of this Agreement, JoVE may, in its sole discretion, elect not take any action with respect to the Article until such time as it has received complete, executed Article and Video License Agreements from each such author. JoVE reserves the right, in its absolute and sole discretion andwithout giving any reason therefore, to accept or decline any work submitted to JoVE. JoVE and its employees, agents and independent contractors shall have full, unfettered access to the facilities of the Author or of the Author's institution as necessary to make the Video, whether actually published or not. JoVE has sole discretion as to the method of making and publishing the Materials, including, without limitation, to all decisions regarding editing, lighting, filming, timing of publication, if any, length, quality, content and the like.

12. **Indemnification.** The Author agrees to indemnify JoVE and/or its successors and assigns from and against any and all claims, costs, and expenses, including attorney's fees, arising out of any breach of any warranty or other representations contained herein. The Author further agrees to indemnify and hold harmless JoVE from and against any and all claims, costs, and expenses, including attorney's fees, resulting from the breach by the Author of any representation or warranty contained herein or from allegations or instances of violation of intellectual property rights, damage to the Author's or the Author's institution's facilities, fraud, libel, defamation, research, equipment, experiments, property damage, personal injury, violations of institutional, laboratory, hospital, ethical, human and animal treatment, privacy or other rules, regulations, laws, procedures or guidelines, liabilities and other losses or damages related in any way to the submission of work to JoVE, making of videos by JoVE, or publication in JoVE or elsewhere by JoVE. The Author shall be responsible for, and shall hold JoVE harmless from, damages caused by lack of sterilization, lack of cleanliness or by contaminationdue to the making of a video by JoVE its employees, agents or independent contractors. All sterilization, cleanliness or decontamination procedures shall be solely the responsibility of the Author and shall be undertaken at the Author's expense. All indemnifications provided herein shall include JoVE's attorney's fees and costs related to said losses or damages. Such indemnification and holding harmless shall include such losses or damages incurred by, or in connection with, acts or omissions of JoVE, its employees, agents or independent contractors. 13. **Fees.** To cover the cost incurred for publication, Jo VE must receive payment before production and publication the Materials. Payment is due in 21 days of invoice. Should the Materials not be published due to an editorial or production decision, these funds will be returned to the Author. Withdrawal by the Author of any submitted Materials after final peer review approval will result in a US$1,200 fee to cover pre-production expenses incurred by JoVE. If payment is not received by the completion of filming, production and publication of the Materials will be suspended until payment is received. 14. **Transfer, Governing Law.** This Agreement may be assigned by JoVE and shall inure to the benefits of any of JoVE's successors and assignees. This Agreement shall be governed and construed by the internal laws of the Commonwealth of Massachusetts without giving effect to any conflict of law provision thereunder. This Agreement may be executed in counterparts, each of which shall be deemed an original, but all of which together shall be deemed to me one and the same agreement. A signed copy of this Agreement delivered by facsimile, e-mail or other means of electronic transmission shall be deemed to have the same legal effect as delivery of an original signed copy of this Agreement.

A signed copy of this document must be sent with all new submissions. Only one Agreement is required per submission.

jove JOURNAL OF VISUALIZED EXPERIMENTS
1 Alewife Center #200
Cambridge, MA 02140
tel. 617.945.9051
www.jove.com

ARTICLE AND VIDEO LICENSE AGREEMENT - UK

CORRESPONDING AUTHOR

Name:	Davor Pavlovic		
Department:	Institute of Cardiovascular Sciences		
Institution:	University of Birmingham		
Title:	Dr		
Signature:	Davor Pavlovic	Date:	07-01-2019

Please submit a **signed** and **dated** copy of this license by one of the following three methods:

1. Upload an electronic version on the JoVE submission site
2. Fax the document to +1.866.381.2236
3. Mail the document to JoVE / Attn: JoVE Editorial / 1 Alewife Center #200 / Cambridge, MA 02140

Dear Editor/Reviewers,

We thank you all for your time and effort in reviewing our manuscript and the accompanying software. Please find below our responses to specific points raised, in blue. Modifications made to the manuscript are quoted and shown in italics. We have submitted a revised manuscript "JoVe resubmission Final" but we also provide a version of the manuscript in track mode "JoVe resubmission track mode".

Editorial comments:

General:

1. Please take this opportunity to thoroughly proofread the manuscript to ensure that there are no spelling or grammar issues.

Protocol:

1. Please ensure that all text in the protocol section is written in the imperative tense as if telling someone how to do the technique (e.g., "Do this," "Ensure that," etc.). The actions should be described in the imperative tense in complete sentences wherever possible.

We have now addressed this throughout the manuscript.

2. For each protocol step, please ensure you answer the "how" question, i.e., how is the step performed? Alternatively, add references to published material specifying how to perform the protocol action. If revisions cause a step to have more than 2-3 actions and 4 sentences per step, please split into separate steps or substeps.

Specific Protocol steps:

1. 3.4 substeps: It's a bit unclear what 'Signal Inversion' etc. are–settings in 'Process Images'? Please clarify.

Sorry, this was unlcear. Yes, these are the settings under the heading 'Process Images'. Step 3.4 has now been revised to clarify this, see below and page 4, lines 164-168.

> *"4. Once an appropriate threshold has been applied, press 'Process Images' to apply processing. Settings for processing are detailed below (3.4.1-3.4.5)."*

Figures:

1. Please obtain explicit copyright permission to reuse any figures from a previous publication. Explicit permission can be expressed in the form of a letter from the editor or a link to the editorial policy that allows re-prints. Please upload this information as a .doc or .docx file to your Editorial Manager account.

Permission to reuse figures has been received, and this information has been uploaded in the document 'Scientific reports permission.docx'

2. Figures 1, 2, and 4L Please include a space between numerals and units; e.g., '200 ms' instead of '200ms'.

Figures have been updated as requested.

References:
1. Please do not abbreviate journal titles.

Reference list updated as recommended.

Table of Materials:
1. Please ensure the Table of Materials has information on all materials and equipment used, especially those mentioned in the Protocol.

Software was developed in Matlab as specified in the manuscript.

Your manuscript, JoVE59663R1 "High-throughput analysis of optical mapping data using ElectroMap: A Matlab based open-source software.," has been editorially reviewed and the following comment needs to be addressed: There is a 'Table 1' mentioned in the manuscript (at the beginning of the discussion), but no such table has been included in the submission. Can you send that to me at this address (or edit the reference out if it's not supposed to be there)?

This has now been corrected.

Reviewers' comments:

Reviewer #1:
Manuscript Summary:
The manuscript includes software for the analysis of optical mapping videos and a protocol describing the use of the software.

Major Concerns:
The title contains "open source software", suggesting that it is immediately available to everyone. Nevertheless, the software is written in Matlab, a commercial software, which is not necessarily available to every researcher and not very widespread among researchers in the life sciences. I would therefore suggest to include "Matlab" in the title, i.e. "... Matlab based open source software", see also "MultiElec: a Matlab based application for MEA data analysis" by V. Georgiadis et al.

We agree that the title should be edited to reflect the fact the software platform is Matlab based. The title has now been updated, see below.

"High-throughput analysis of optical mapping data using ElectroMap: A Matlab based open-source software."

Please note that for users that do not have access to MATLAB, we also provide a standalone .exe version of the software at https://drive.google.com/open?id=1nJyl07w9WIt5zWcit0aEyIbtg31tANxI. This can be run without owning MATLAB license, and instructions for using this are outlined in the section 2 subsection 'Setup 2: Standalone .exe file' (page 4, Lines 132-141).

Furthermore, the title contains "high-throughput". The authors should specify what they mean by "high-throughput" as Matlab is relatively slow in comparison to other languages such as for instance C/C++.

Our main objective is to make a 'high-throughput' software with a graphical user interface-platform that is flexible and allows batch processing of entire experimental files. In addition, we have compared our software to previously published algorithms and shown substantially improved processing speeds[1]. This is combined with automated pacing frequency detection (Figure 4), a range of signal segmentation options (Section 4) and functionality for automated analysis of entire datasets (Step 7.2). It is correct that migration of the software to languages such as C/C++ would further enhance computation speed, and so is an attractive next step in development, however we believe the current developments made within the software justify the use of 'High-throughput'.

The abstract should mention that the toolbox can only be used to process video data obtained with uncoupled hearts.

We agree that for fully accurate analysis of repolarisation/decay in optically mapped datasets mechanical uncoupling is required. However, we do not feel that this should be added to the abstract. Activation analysis can still be performed in large areas of tissue where contraction persists (Figure 5). Additionally, although not the focus of the current manuscript, we have utilised ElectroMap for analysis of virtual electrogram signals acquired *in vivo* from freely beating hearts[1].

The use of the software is not easy and the protocol should be improved to make it easier for beginners. All necessary source code was provided on GitHub. Downloading and running ElectroMap worked as described (in this case using Matlab 2017b). Also, loading one of my own .mat files containing an optical mapping video worked fine, the first video frame was segmented automatically after loading. However, from there on things got tricky. The user interface is quite elaborate and not easy to understand with limited time (1 hr). I would therefore suggest to include screenshots showing the buttons and tasks described in the different steps in sections 3.3ff. Two example files were provided. I would suggest to mention this in section '3. Image loading' and then advice users to perform all following steps using these files. For instance: 1. Load file 'xyz' (by doing ...). 2. Perform pre-processing to obtain a specific goal (i.e. remove noise) by clicking here and there (with screenshot), etc. Walk users through a step-by-step tutorial. With the way the protocol is written at the moment it is a bit

difficult to understand the structure of the software and the intentions of the analysis, and I believe a step-by-step tutorial with screenshots illustrating each step would decrease the learning threshold quite a bit. I would therefore suggest to revise the protocol accordingly.

We agree that a step by step guide including screenshots, for section 3, is a useful resource. Step-by-step guide (with screenshots) is now available for download, named as 'ElectroMap Basic Analysis and Mapping Workflow.pdf', at https://github.com/CXO531/ElectroMap.

Overall it seems that the software was designed for very specific tasks, i.e. APD, activation time and conduction velocity measurements during regular cardiac activity and an analysis of alternan activity. While the first ones are very general tasks, the latter is very specific. However, there are other very general tasks that seem to be missing: analysis of arrhythmias, i.e. phase singularity detection and tracking. I would suggest to highlight this focus in the introduction and mention what the software offers and does not seem to provide.

ElectroMap has been designed to calculate and map a multitude of EP parameters, including: APD, activation time, amplitude, diastolic interval, dominant frequency, time to peak, signal to noise ratio and relaxation constant. It also contains standalone modules for calculation of conduction velocity using a number of methodologies, and further modules for regional AP/CaT interrogation/comparison and calculation and mapping of alternans.

We agree that phase singularity detection and tracking as well as several other functionalities/features (dual/ratiometric dye processing and motion artefact correction) would be valuable additions to the software, and now highlight this in our discussion, see pages 13-14, lines 568-578.

> *"At present, ElectroMap does not support removal of motion artefacts from raw data in the same manner as baseline correction. Therefore, a possible future development of the software is inclusion of motion artefact removal by computational methods as has been reported[2,3]. Furthermore, ElectroMap is currently limited to study of one optical signal. However, for ratiometric dyes and simultaneous use of voltage and calcium dyes[4], concurrent processing of two wavelength channels is required. The integration of dual signal analysis is therefore an important future addition to the software. Extension of analysis options applicable to arrhythmic datasets, such as phase singularity tracking, would equally broaden the scope of the software[5,6].*

It was not possible for me to find out whether the software can play the (raw or processed) videos. This is quite an essential functionality and should be available immediately when aiming to analyse optical mapping data. If not present, I would suggest to implement a play button. It seems that currently videos can only be played after they were exported from Matlab.

We agree! This would be an extremely useful feature and we will add to future releases. Raw videos can be exported from the software by pressing 'Raw Videos' once datasets have been

processed, but as suggested are not immediately available to the user within the interface which would be beneficial.

I would also suggest to simplify the graphical user interface.

On this point, we would like to emphasise that processing, analysis and mapping of optical mapping data requires understanding of the multitude of processing options and hence we do not advocate hiding these essential user-modifiable parameters. Making these options immediately available and modifiable rather than hidden, combined with the ability to save settings for future use, aids understanding of the effects these parameters have on quantification of optical mapping datasets.

Reference 20 is not yet published and can not be evaluated. In line 84 the authors write "We have recently published and released a comprehensive software platform." citing 20. Access to this publication would be crucial for the evaluation of this manuscript.

This reference (13 in updated manuscript) has now been published (O'Shea et al 2019, Scientific Reports. 9:1389)[1]

Overall, the software can certainly be very useful to some researchers, but it is not very versatile and provides only very specific functionality.

Minor Concerns:
The references provided regarding optical mapping seem a bit arbitrary. Standard literature is not mentioned.

Reference list has now been expanded, and we believe currently gives a good overview of optical mapping, its use in a wide variety of experimental preparations and processing and analysis of optical mapping datasets.

We thank the reviewer for helping to improve the manuscript and are happy to take suggestions from the reviewers and editor if they feel any other particularly pertinent literature is currently missing.

The references should include Laughner et al. "Processing and analysis of cardiac optical mapping data obtained with potentiometric dyes."

We apologise for this omission, we completely agree that this is an essential study and have now added the reference as suggested.

In line 75 the authors write: "To overcome these limitations, several research groups have designed custom processing pipelines tailored towards their experimental model, question and hardware7." and provide only 1 reference. Ideally references to these several research groups would be provided here. It is also not clear how the work in reference 7 relates to the statement and the entire paragraph, do they provide algorithms?

Further examples of the use of custom algorithms have been added (see references 7 and 14-16).

The point that we tried to make is that, many groups will have designed tailor-made algorithms to be used in-house and not necessarily shared. Indeed, in the questioned reference (Reference 7, Yu et al 2014 Prog Biophys Mol Biol. 115(2-3):340-8.), algorithms are developed for analysis of optical mapping data from isolated murine atria. These algorithms were custom made for a newly designed setup, tailored towards murine atria and the code/software to perform this analysis was not freely provided.

Reviewer #2:

Manuscript Summary:

In their manuscript O'Shea et al. provide a detailed protocol for using the recently developed open-source software platform ElectroMap, which was designed for analyzing cardiac optical mapping data. The software package allows for high-throughput analysis of action potential frequency and beat-by-beat variability as well as automated signal averaging. Custom modules furthermore enable quantification of conduction velocity and alternans. The manuscript is very well written and provides step-by-step guidance for data analysis, including installation of the software, data processing, use of specialized analysis tools and data export functions. The manuscript also includes a short section wherein current limitations of the software are explained.

We thank the reviewer for their positive remarks about the manuscript and associated software.

Major Concerns:

The reviewer does not recognize any major concerns regarding the provided protocol.

Minor Concerns:

The cross references to other steps in the protocol are sometimes misleading. For example in point 3.2 the sentence "In this case, please skip step 3.1" is not clear to me. Are steps and sections on the same level of hierarchy? If possible, it might be useful to not have a step/option 3 under 3, but to use 3.3 instead, and 3.4.1 for the lowest level.

Thank you for spotting this error. This should indeed read 'In this case, please skip step **3.3'** and has been updated (page 4, Line 153).

Point 3.4.1: Is there an option to process ratiometric data at all? This might be a very useful option. If currently not possible, it would be nice to mention this option when discussing current limitations.

At present, ElectroMap is setup for only one optical signal and so cannot process ratiometric signals unless the data has already been collapsed. We agree that analysis of these datasets, and others comprising of multiple optical signals such as dual voltage-calcium dye

experiments, would be very useful and is part of our current and future developments. We have therefore expanded our discussion on the addition of these features to the software, see below and page 14, lines 570-573.

> *"Furthermore, ElectroMap is currently limited to study of one optical signal. However, for ratiometric dyes and simultaneous use of voltage and calcium dyes[4] concurrent processing of two wavelength channels is required. The integration of dual signal analysis is therefore an important future addition to the software."*

Point 3.4.1: "optically paced datasets". You may want to add a sentence on combined optical mapping and optogenetic activation in the introduction, since many readers might not be familiar with the concept of optical pacing.

We agree! Introduction (page 2, lines 74-77) and subsection 3.4.5 has now been expanded to briefly introduce the concept of optogenetic pacing to the reader (page 5, lines 194-197), and a further reference to these techniques has been provided.

Point 5.4: APD start time: How is this defined? Could one use dV/dt max as a start time for APD calculations? Please further explain.

APD start time can be set to one of four options, and dV/dt is used as default within the software. We have now expanded point 5.4 to make this clear, see below and page 7, lines 268-272.

> *'APD' Start time - Start time for duration measurements. These are the same options for deciding the activation time for isochronal maps (discussed below) and are termed: Start (d^2F/dt^2_{max}), Upstroke (dF/dt_{max}), Depolarisation midpoint (time of 50% amplitude), Peak (time of maximum amplitude). These definitions applied to mouse and guinea pig action potentials are shown in Figure 2A.*

Figure 1A: Please provide a high-resolution image. 1D: Please label quantified parameters (blue, green, red) on right hand side. Please also ensure aligned labels and line width of scale bars for all figures.

This has now been implemented.

Figure 2A: The peak (green cross) is shown in legend, but not labelled in the AP data.

We have now labelled the peak as advised.

Figure 3: Do the shown AP traces represent beats for the entire image and if yes, are the time courses for each pixel aligned to the time point of peak amplitude? Please add an explanation to the figure legend.

The peaks represent a single pixel data, and this is now clearly stated in the legend of Figure 3.

Figure 4A: Could you please show a screenshot wherein the unit (ms) is fully visible for the

cycle duration? 4B: Please correct: Cycle Length on both axes.

This has now been done. Many thanks for spotting and we would like to thank you for the suggestions to improve the quality of the figures.

Reviewer #3:

Manuscript Summary:

O'Shea et al. propose a software user interface for the visualization and analysis of universal optical mapping data. The software is based on the Matlab platform and offers an open-source dissemination of the code. Installation and code-access promise to be easy and transparent. The software boasts an array of analyses options that mark clear experience of the creators in optical mapping. The manuscript however requires some clarifications and transparency are however needed concerning the software functions and modules during post processing and analyses for the lay user that would not be familiar with the code itself. These concerns are detailed below.

Major Concerns:

Currently lacking is a detailed description of each function. Information lacking throughout includes descriptions of whether post processing occurs on a pixel-by-pixel basis or considers the whole frame, which functions implement inbuilt Matlab functions and which are custom built. A point-by-point section describes the specific questions raised:

We thank the reviewer for their comments, the technical description of the functions is presented in our manuscript published recently (reference 13 in updated manuscript, O'Shea et al 2019, Scientific Reports. 9:1389) whereas this present manuscript focuses on the use of the software. Regarding post-processing on a pixel-to-pixel or whole image basis, this is now stated. For example, with baseline correction (4.3). Alignment for ensemble averaging (discussed further below) is currently based on peak in the whole tissue signal. All other post-processing is performed on each individual pixel independently.

Line 146 : Please clarify the thresholding applied. Is this a simple intensity cut-off or related to the amplitude of signals ? If based on background intensity, does it suppose that the first frame occurs during rest ? Is the same resultant mask then applied throughout the whole acquisition ? Or is this recalculated for each frame?

Apologies for not making this clear. There are two options for application of thresholding. The default option is based on the pixel intensity of the first frame, but the user can instead choose to threshold based on the time-course signal amplitude. We have now expanded step 3.2 to makes this clearer, see below and page 4 lines 153-156. Please note that once the thresholding is selected, it is then applied to the whole image stack.

> *"As default, thresholding is based on the pixel intensities in the first frame. However, this can be modified to threshold based to the signal time course amplitude by changing the option in the 'Image for threshold' dropdown menu. Please note that once the thresholding is selected,*

it is then applied to the whole image stack."

Line 154 : Is there a prompt to complete this important step ? The complex interface layout does not otherwise make this a clear and necessary step. It is also not clear why thresholding and applications of ROI functions require either the spatial or temporal resolution to complete these computations, which should only require the image pixel coordinates, when considering these raw functions alone ; hence the suggestion to include some kind of prompt.

We thank the reviewer for detailed feedback on the current software. This is a first release version that we hope to continue to improve now that it can be utilised by a wider audience, and such feedback is invaluable to help us achieve an improved software.

There is not a prompt for this step currently. However, the 'Process Images' button is greyed out until the point where the images have been loaded, and 'Produce Maps' button does not become active until the images have been fully processed. We also provide a user manual at https://github.com/CXO531/ElectroMap.

The reviewer is correct, spatial or temporal resolution is not required to use the ROI functions which are applied by selecting 'Load Images' (Steps 3.2 to 3.3). The need for correct resolution input is first mentioned in point 3.4 which pertains to selecting 'Process Images' once the ROI has been selected.

Line 169 : I would have expected top-hat filtering in the temporal domain to be considered a filtering or smoothing function, rather than baseline correction. I am assuming that the kernel is relatively short (extending over 3-9 frames).

The use of the terms 'Top-hat filtering/filter' in this section was indeed misleading, and hence the phrasing has been modified to refer to 'Top-Hat correction' or 'Top-Hat Kernel'. For the purposes of baseline correction, we apply a long kernel length and subtract the resulting trace. We have previously shown how this method can be effective compared to polynomial based techniques[7]. Section 4.3 has been updated to improve clarity on this point, below and page 5, lines 179-184.

> *"4.3 Baseline correction: Top-hat[8] or polynomial (4^{th} or 11^{th} degree) correction[9]. Correction can be applied to each pixel individually (long processing time) or as an average of the entire image (quicker but assumes homogenous baseline alterations). Top-hat correction can also be modified by setting the 'Top-Hat Length' in milliseconds, adjacent to the baseline selection dropdown menu. The length of the Top-Hat kernel should be greater than the timescale of the individual action potentials/calcium transients."*

Figure 1 shows examples of filtering applied, but no details are given in the figure or legend to explain which filtering options were applied or the history of processing to each trace.

> Filtered traces shown in Figure 1 are for demonstration purposes only to show the functions that can be applied on selecting 'Process Images' within ElectroMap, and hence full details of particular filter options used here (chosen from the interface) are

not included. We have, however, modified the Figure 1 legend to help clarify a number of processing options.

Line 179 : Removing frames leads to a non-regular grid of the image array. How is this handled for the subsequent processing steps?

To minimise effects of discontinues, all the 'removed frames' are replaced with the frame immediately preceding the section that has been removed. However, although preventing discontinues in the signal, this procedure can still lead to step-like changes in intensity at the end of the removed sections. Hence, where possible, temporal filtering is not advised in this case as now highlighted in the text (below, and page 5, lines 195-197).

> *"NOTE: As frame removal will potentially introduce unphysiological step changes into the image signals, temporal filtering may introduce artefacts to the data and so is not recommended here."*

Line 190 : References to traces should indicate which figure they are referring to or if it is a general comment directed to the software interface layout.

This trace is now referenced (below and page 5, lines 205-206).

> *"1. Once the file has been processed, peaks in the tissue averaged signal (bottom right trace, Figure 1A) are detected and labelled by red circles."*

Line 190 : Using signal peaks for AP alignment will be robust for APs of small rodents, but the peak is not always so definitively in the same moment during the AP of large mammalian tissue whereby the peak often lies during the plateau phase or close to the square-off upstroke peak as in the guinea pig AP in figure 2. Are other approaches available ? If not, a limitation should be stipulated.

We agree! Alignment based on the whole frame peaks will not always be ideal. We are currently working on updating the software to include the alignment based on dv/dt and from specific regions of interest. We are working on optimising these features and will implement this in future releases.

Line 188 section 4. Are all data segmentation and ensemble averaging functions applied on a pixel-by-pixel basis, or do functions treat the frames as a whole ?

We agree that the ability to apply these features on a pixel to pixel basis would be beneficial, and we plan to implement this in future release.

Line 250 : The parameter term « Duration » is misleading for a parameter that defines the percentage of repolarization. Duration is not even directly measured from this value, which is

actually repolarization time. As it must first be subtracted by the activation time to obtain duration.

As the software allows activation time to be set at peak (max depolarisation point) but also dv/dt, depolarisation midpoint as well as d^2v/dt^2, we decided to use the term 'Duration' rather than repolarisation. In other words, depending on APD start time chosen, the measured APD will consider sections of both the depolarisation and repolarisation phases of the action potential. Furthermore, the software can be used to measure both voltage and calcium signals, making 'Repolarisation %' misleading, in our view.

Part 3 of additional analyses and modules : If I understood correctly, a type of measure missing concerning alternans refers to APD alternans. Here, the APD is typically measured and compared between odd and even beats. This allows for assessment of the spatial distribution of alternans and their concordance/discordance.

Apologies for not making this clear. APD alternans are already measured within our software (see Figure 7 and Supplementary Figure VII in O'Shea et al 2019, Scientific Reports. 9:1389)[1]. APD alternans are detailed in section 3.1 of 'Additional analyses and modules'. We have now expanded this section to give more detail of these measurements, see below and page 9, lines 373-379.

> *"3.1. Duration alternans are measured by comparing the duration measurement from one peak to the next. I.e. if peak one and two and APD_1 and APD_2 respectively, then the duration alternan (ΔAPD) is calculated as*
>
> $$\Delta APD = |APD_1 - APD_2| \qquad (3).$$
>
> *The duration measurement is performed using the settings in the main interface."*

Line 417 : It is reported that part of ElectroMaps flexibility includes camera type. Yet this is never explained. Does this mean, for example, that the software can handle differing image dimensions, resulting from various camera chip pixel sizes (currently available up to 256 pixels in any one direction) and shapes (square/rectangular).

Yes, the software can handle different image dimensions and shapes. We have internally tested and analysed data from the following cameras with varying dimensions and maximal resolutions –

- ORCA Flash 4.0 (cmos camera) – 2048x2048 pixels.
- MiCAM Ultima (cmos camera) – 100x100 pixels.
- Evolve Delta (EMCCD camera) – 512x512 pixels.
- Evolve 128 (EMCCD camera) – 128x128 pixels.

This has now been explicitly stated in section 1.1, see below and page 3, lines 102-108.

> *"Provided that data obtained can be converted to a tiff stack or saved in a .MAT file, it should be analyzable using ElectroMap. This includes data of varying dimensions (square/rectangular) and resolutions (maximum tested 2048x2048 pixels)."*

Reviewer #4:

Manuscript Summary:

The paper on ElectroMap is a useful contribution for research investigators analyzing optical mapping data, because of the many measured parameters and data processing options allow the software to examine data from many sources and imaging modalities. Overall, the approach is applied to cardiac data, but is general enough to be useful for mapping data from other excitable cells (e.g., neural data).

Major Concerns:

The paper would benefit by addressing the following points regarding user interface and program operation.

1) The description of the operation of the user interface is incomplete. In particular,

-- the phase mapping and activation points buttons are not discussed.

We apologise, these options are now discussed:

Activation points (page 7, lines 277-280)

> *"5. Conduction velocity is also measured automatically within the main software interface. This is achieved using the multi-vector method of Bayly et al[10] from the isochronal map defined by the chosen activation measure (discussed in 5.4). Press 'Activation Points' to render a 3D representation of the activation map."*

Phase Mapping (page 10, lines 408-411)

> *"4. Press 'Phase Map' to initiate the phase mapping module. A hilbert transform is performed to calculate the instantaneous phase (between -π and +π) of the signals at each timepoint. Press play or drag slider to visualize phase behavior over time and click on a pixel to render phase diagram."*

-- SNR options are not discussed.

SNR is now discussed (page 7, lines 299-301).

> "9. SNR is calculated as the ratio of the maximum amplitude compared to the standard deviation of the signal at baseline. This analysis is performed post all processing steps. Press 'SNR calculation' in the top menu to edit settings for the period of the signal defined as baseline."

-- what does "fitting activation" in "isochronal and local conduction velocity" box do?

Fitting activation time input instructs the software to apply local vector analysis to the chosen activation time range. Default is 'Full Range' so the analysis is performed on all pixels in the activation map. However, this can be restricted to a custom range of activation times. This setting is now discussed in step 5.6.

"6. The multi-vector conduction velocity measurement method spatially segments the isochronal map into regions of n x n pixels. The value of n can be set by the 'Local Window Size' input, while the range of activation times to apply analysis to can be set using the 'Fitting activation times' inputs."

2) In Figures 3 and 4: what do n values refer to? Recordings or different hearts?

n numbers refer to hearts. This has now been explicitly stated in the figure legends.

3) Can the data files used to create the figures be provided (e.g., Fig. 3 - mouse atria paced at 3 Hz and 10 Hz; Fig. 4 -decreasing CL)?

Example files from these datasets have been uploaded to https://drive.google.com/open?id=1nJyI07w9WIt5zWcit0aEyIbtg31tANxI. These have been labelled '10-12.5-3Hz.tif and 'decreasingCL.tif' respectively. 12.5Hz pacing was not used for data presented in figure 3.

4) The module for alternans analysis is a key part of the program, please include a figure and data showing such analysis.

We agree that alternans analysis is an important feature. The alternans module has been outlined in detail in our recent publication and we now refer to this in section 7.3 and 7.3.1 (see Figure 7 and Supplementary Figure VII in O'Shea et al 2019, Scientific Reports. 9:1389)[1].

5) The following observations/questions result from analyzing the included atria.tif file with the atria settings, unless otherwise noted:
-- Dominant frequency values appear to be wrong by a factor of 2.

The range for dominant frequency settings in the ElectroMap version on GitHub is automatically set to 4-10 Hz, hence why in your analysis 3 Hz has been excluded. The user can therefore set the range as detailed in section 7, step 1.2. We have now, however, changed the default to 0.5-10Hz in the latest version uploaded on GitHub.

-- Segment video produces an error:
Error using waitbar (line 111)
Improper arguments for waitbar.
Error in ElectroMap>pushbutton17_Callback (line 2605)
waitbar((0.1+0.9*(i/numsec)),wb,'Producing video file');
Error in gui_mainfcn (line 95)
feval(varargin{:});
Error in ElectroMap (line 58)
gui_mainfcn(gui_State, varargin{:});
Error in
matlab.graphics.internal.figfile.FigFile/read>@(hObject,eventdata)ElectroMap('pushbutton17_Callback',hObject,eventdata,guidata(hObject)

Caused by:
Error using matlab.graphics.primitive.Text/set
Invalid or deleted object.

Yes, we have also encountered an error when pressing 'Segment Video'. Thank you for bringing this to our attention, and we will endeavour to rectify as soon as possible.

-- Why does a figure appear when remove frames is checked?

-- When analyzing atria data, remove frames creates a notch in the upstroke - why?

The remove frames option is currently designed to remove light pacing peak frames which are assumed to have a much greater amplitude than the signal of interest. The figure shows the peaks that have been identified to be removed. Hence, it is not currently useful in data such as 'atria.tif', where no such pacing peaks are present. This feature will however be expanded in future releases to allow more control over frame removal.

-- Changing Spatial filtering kernel seems to have no effect, even when switching between "none" and "average" filter with size=90 and sigma=90.

We applied various spatial filters to the atria.tif file and observed changes in the processed signals and resulting APD50 maps, see Figure R1. On changing the spatial filter, 'Process Images' was pressed to apply the new settings to the image stack before selecting 'Produce Maps' to quantify APD.

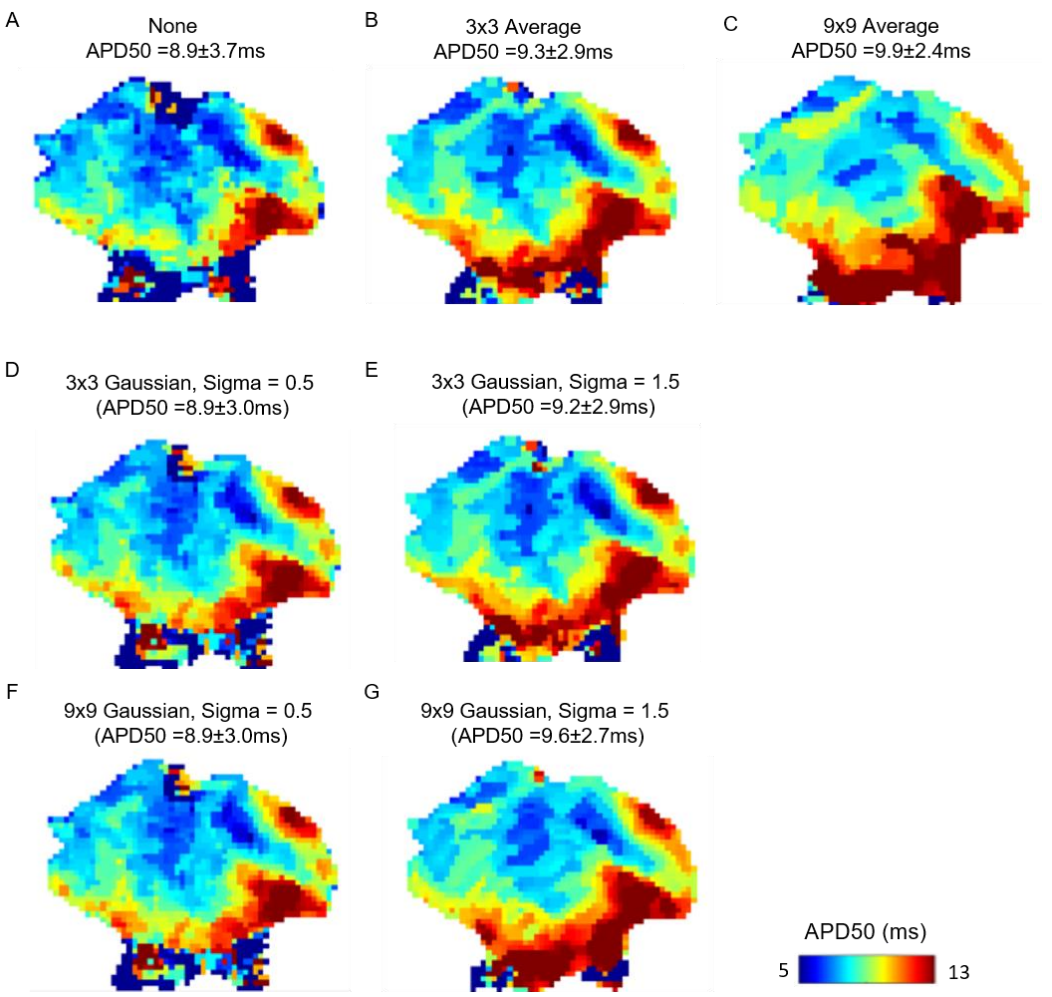

Figure R1: APD50 maps generated from murine left atria following application of spatial filters. A) No spatial filtering. B&C) Average Filtering of 3x3 (B) and 9x9 (C) pixels respectively. D-G) Gaussian Filtering with varying kernel size and standard deviations (Sigma).

6) A key advantage of this software is the ability to use it on many kinds of data, including data formats. However, our x-y-t .mat images did not load correctly. Please include an example of .mat data that can be analyzed by the program.

.MAT version of 'atria.tif' example file has been uploaded to https://drive.google.com/open?id=1nJyI07w9WIt5zWcit0aEyIbtg31tANxl. Please bear in mind that for use in ElectroMap, .MAT files must contain only one variable, ie. the image stack.

Minor Concerns:

1) As several suggestions,

-- The ability to display first and 2nd derivatives, as done in Fig. 2, would be useful, as well as a discussion of how these are calculated.

-- it may be better to have diastolic interval use the values in the signal processing box for APD%, activation time, etc. rather than being fixed at APD90.

-- in comparing pixels, it would be helpful for "normalize" to instantly have the effect, rather than having to check it before choosing points.

These are all valuable suggestions and we thank the reviewer for their input. The current version is a first release software, and we aim to explore and add community requested features such as those suggested to the software in future releases.

References

1. O'Shea, C. *et al.* ElectroMap: High-throughput open-source software for analysis and mapping of cardiac electrophysiology. *Scientific Reports* **9,** 1–13 (2019).
2. Khwaounjoo, P. *et al.* Image-Based Motion Correction for Optical Mapping of Cardiac Electrical Activity. *Annals of Biomedical Engineering* **43,** 1235–1246 (2014).
3. Christoph, J. & Luther, S. Marker-Free Tracking for Motion Artifact Compensation and Deformation Measurements in Optical Mapping Videos of Contracting Hearts. *Frontiers in Physiology* **9,** (2018).
4. Jaimes, R. *et al.* A technical review of optical mapping of intracellular calcium within myocardial tissue. *American Journal of Physiology - Heart and Circulatory Physiology* **310,** H1388–H1401 (2016).
5. Umapathy, K. *et al.* Phase Mapping of Cardiac Fibrillation. *Circulation: Arrhythmia and Electrophysiology* **3,** 105–114 (2010).
6. Tomii, N. *et al.* Detection Algorithm of Phase Singularity Using Phase Variance Analysis for Epicardial Optical Mapping Data. *IEEE Transactions on Biomedical Engineering* **63,** 1795–1803 (2016).
7. Yu, T. Y. *et al.* Optical mapping design for murine atrial electrophysiology. *Computer Methods in Biomechanics and Biomedical Engineering: Imaging & Visualization* **5,** 368–378 (2017).
8. Yu, T. Y. *et al.* Optical mapping design for murine atrial electrophysiology. *Computer Methods in Biomechanics and Biomedical Engineering: Imaging and Visualization* **5,** 368–376 (2017).
9. Laughner, J. I., Ng, F. S., Sulkin, M. S., Arthur, R. M. & Efimov, I. R. Processing and analysis of cardiac optical mapping data obtained with potentiometric dyes. *AJP: Heart and Circulatory Physiology* **303,** H753–H765 (2012).
10. Bayly, P. V *et al.* Estimation of Conduction Velocity Vector Fields from Epicardial Mapping Data. **45,** 563–571 (1998).

From: <journalpermissions@springernature.com>
Date: 15 February 2019 at 16:26:53 GMT
To: Davor Pavlovic <D.Pavlovic@bham.ac.uk>
Subject: RE: Request for permission to reproduce the figures

Dear Davor,

Thank you for your email. This work is licensed under a Creative Commons Attribution 4.0 International License, which permits unrestricted use, distribution, and reproduction in any medium, provided you give appropriate credit to the original author(s) and the source, provide a link to the Creative Commons license, and indicate if changes were made. **You are not required to obtain permission to reuse this article.** The images or other third party material in this article are included in the article's Creative Commons license, unless indicated otherwise in the credit line; if the material is not included under the Creative Commons license, users will need to obtain permission from the license holder to reproduce the material. To view a copy of this license, visit http://creativecommons.org/licenses/by/4.0/.

Best wishes,
Oda

Oda Siqveland
Rights Executive

SpringerNature
The Campus, 4 Crinan Street, London N1 9XW,
United Kingdom
T +44 (0) 207 014 6851

TITLE:

High-Throughput Analysis of Optical Mapping Data Using ElectroMap: A Matlab based open-source software.

AUTHORS & AFFILIATIONS:

Christopher O'Shea[1,2,3], Andrew P Holmes[1,4], Ting Y Yu[1], James Winter[1], Simon P Wells[1], Beth A Parker[1], Dannie Fobian[1], Daniel M Johnson[1], Joao Correia[5], Paulus Kirchhof[1], Larissa Fabritz[1], Kashif Rajpoot[3], Davor Pavlovic[1]

[1]Institute of Cardiovascular Sciences, University of Birmingham, UK
[2]EPSRC Centre for Doctoral Training in Physical Sciences for Health, School of Chemistry, University of Birmingham, UK
[3]School of Computer Science, University of Birmingham, Birmingham, UK
[4]Institute of Clinical Sciences, University of Birmingham, UK
[5]Institute of Microbiology and Infection, School of Biosciences, University of Birmingham, UK

Corresponding Authors:

Davor Pavlovic (d.pavlovic@bham.ac.uk
Kashif Rajpoot (k.m.rajpoot@bham.ac.uk)

Email Addresses of Co-authors:

Christopher O'Shea (CXO531@bham.ac.uk)
Andrew P Holmes (A.P.Holmes@bham.ac.uk)
Ting Y Yu (tingyueyu@gmail.com)
James Winter (J.Winter.1@bham.ac.uk)
Simon P Wells (SXW113@student.bham.ac.uk)
Beth Parker (BAP676@student.bham.ac.uk)
Dannie Fobian (DXF608@student.bham.ac.uk)
Daniel M Johnson (D.M.Johnson.1@bham.ac.uk)
Joao Correia (j.correia@cairn-research.co.uk)
Paulus Kirchhof (P.Kirchhof@bham.ac.uk)
Larissa Fabritz (L.Fabritz@bham.ac.uk)

KEYWORDS:

cardiac optical mapping, software, electrophysiology, arrythmia, fluorescent sensors, action potential, calcium

SUMMARY:

This protocol describes the setup and use of ElectroMap, a MATLAB-based open-source software platform for analysis of cardiac optical mapping data. ElectroMap provides a versatile high-throughput tool for analysis of optical mapping voltage and calcium datasets across a wide range of cardiac experimental models.

ABSTRACT:

Optical mapping is an established technique for high spatio-temporal resolution study of cardiac electrophysiology in multi-cellular preparations. Here we present, in a step-by-step guide, the use of ElectroMap for analysis, quantification, and mapping of high-resolution voltage and calcium datasets acquired by optical mapping. ElectroMap analysis options cover a wide variety of key electrophysiological parameters, and the graphical user interface allows straightforward modification of pre-processing and parameter definitions, making ElectroMap applicable to a wide range of experimental models. We show how built-in pacing frequency detection and signal segmentation allows high-throughput analysis of entire experimental recordings, acute responses, and single beat-to-beat variability. Additionally, ElectroMap incorporates automated multi-beat averaging to improve signal quality of noisy datasets, and here we demonstrate how this feature can help elucidate electrophysiological changes that might otherwise go undetected when using single beat analysis. Custom modules are included within the software for detailed investigation of conduction, single file analysis, and alternans, as demonstrated here. This software platform can be used to enable and accelerate the processing, analysis, and mapping of complex cardiac electrophysiology.

INTRODUCTION:

Optical mapping utilizes fluorescent reporters of voltage and/or calcium concentration to interrogate cardiac electrophysiology (EP) and calcium handling in multicellular preparations, with greater spatial resolution than achievable with traditional techniques[1–3]. Therefore, optical mapping has emerged as an important and ever increasingly utilized technique, providing key insights into physiological and pathophysiological electrical behavior in the heart[3–8]. Effective processing and analysis of data obtained from optical mapping experiments is complicated by several factors. The high spatiotemporal resolution nature of optical mapping datasets results in raw videos files composed of thousands of image frames, each made up of a number of individual pixels, giving rise to large data files that necessitate high-throughput and automated processing[9]. Small pixel sizes, poor and uneven dye loading and small fractional changes in fluorescence result in optical signals with low signal to noise ratio (SNR), requiring pre-processing before effective analysis is achievable[10]. Processing and analysis can be further complicated by the use of optogenetic pacing protocols which utilize light to initiate activation, potentially distorting the recorded signal from the fluorescent sensors[11,12]. Furthermore, once data has been processed, several non-consistent techniques and definitions can be applied to measure parameters of interest, with the most applicable techniques varying depending on experimental setup, model and question[2,10,13]. These limitations prevent further uptake of the technology and hinder truly objective analysis.

To overcome these limitations, several research groups have designed custom processing pipelines tailored towards their experimental model, question and hardware[7,14–16]. Others utilize commercial proprietary software where the underlying algorithms may be difficult to access[4,17]. As a result, there is a clear need for a freely available open-source software platform for processing and analysis of optical mapping data. It is important that this software is open-source, easy to use, flexible to parameter adjustment, applicable to a range of experimental models with distinct EP properties and crucially allows straightforward and tunable quantification of the range of cardiac parameters that can be studied using optical mapping.

We have recently published and released a comprehensive software platform, ElectroMap, for high-throughout, semi-automated processing, analysis and mapping of cardiac optical mapping datasets[13]. Here, we present a video manual for the utilization of ElectroMap and demonstrate how it can be used to process, analyze and map several optical mapping datasets. We focus on the use of ElectroMap to quantify standard EP and calcium handling variables and demonstrate the use of standalone conduction velocity, single file analysis and alternans modules.

PROTOCOL:

1. Optical mapping data collection

1.1. Perform cardiac optical mapping using one of a wide range of experimental models including intact and isolated whole hearts[6,18], isolated atria[14,19], ventricular wedges[20], cardiac slices[21,22], and cellular monolayers[23]. See associated references for experimental designs to collect raw optical mapping data from these preparations. Provided that data obtained can be converted to a tiff stack or saved in a .MAT file, it should be analyzable using ElectroMap. This includes data of varying dimensions (square/rectangular) and resolutions (maximum tested currently 2048 pixels x 2048 pixels).

2. Software installation and start-up

NOTE: Below are detailed the two methods for installing and running ElectroMap – either within MATLAB run from the source (.m) code or as a standalone executable file (.exe for windows). The final software and its functionality are invariant between the two setup options (other than a few differences in directory navigation). Therefore, the main considerations for choosing version to install are access to MATLAB and required toolboxes and whether access to source code is desired. Where possible, it is recommended to use the MATLAB version for faster start up times, shorter processing times, and easier error reporting.

2.1. Setup 1: Running electromap within MATLAB

2.1.1. Install MATLAB. ElectroMap was designed in MATLAB 2017a, however, software has been tested for use in all subsequent releases of MATLAB (up to 2018b at time of writing). The following toolboxes are required: Image Processing, Signal Processing, Statistics and Machine Learning, and Curve Fitting.

2.1.2. Download/clone **all** files from the latest 'source code' release of ElectroMap from the GitHub repository (https://github.com/CXO531/ElectroMap). Unzip the downloaded contents to a desired location.

2.1.3. Open MATLAB and navigate to the folder location hosting the ElectroMap source code. Then, open the file **ElectroMap.m** and press run in the editor, or alternatively type **ElectroMap**

in the command window and press **RETURN**. This will start the ElectroMap user interface, **Figure 1A**.

2.2. Setup 2: Standalone .exe file

2.2.1. Download the installer file: https://drive.google.com/open?id=1nJyI07w9WIt5zWcit0aEyIbtg31tANxI.

2.2.2. Follow the instructions in the installer, which will download required the MATLAB runtime from the web alongside ElectroMap software.

2.2.3. Run **ElectroMap.exe**.

NOTE: Start up time for the standalone version can be several minutes.

3. Image loading and pre-processing

3.1. Press **Select Folder** and navigate to the location of the data file(s) to be analyzed. This will populate the left-hand listbox with all files within that directory that are of the correct file type (.tif or .MAT). .MAT files must only contain the image stack variable.

NOTE: Only folders and not individual files will appear as you navigate through the directory selector.

3.2. Select file to be loaded from within the interface and press **Load Images**.

3.2.1. Once loaded, the first frame will appear, and the red outline will indicate automatic thresholding of the image. If needed, reload previously used ROIs by selecting **Save/Load ROI**. In this case, skip step 3.3.

3.2.2. As default, thresholding is based on the pixel intensities in the first frame. If desired, modify this to a threshold based to the signal time course amplitude by changing the option in the **Image for threshold** dropdown menu. Please note that once the thresholding is selected, it is then applied for the whole image stack.

3.3. If desired, change the threshold option to **manual**, which will activate the slider to manually adjust the image threshold. Additionally, crop images (**Crop Image**) and/or draw a custom region of interest (**Custom ROI**) for analysis by selecting the appropriate tick box(es) below threshold options. Note that advanced options for region of interest selection such as number of areas are available from **ROI Selection** from the top menu.

3.4. Once an appropriate threshold has been applied, press **Process Images** to apply processing. Settings for processing are detailed below (step 3.4.1-3.4.5). At this point, ensure that that the correct camera settings have been entered. These are **Pixel Size** in µm (IMPORTANT: this is the

image pixel size, and not the size of the pixels that make up the chip or equivalent hardware in the imaging device) and **Framerate** in kHz.

3.4.1. For signal inversion, tick the **Invert Data** checkbox to enable. If reported fluorescent signal is inversely proportional to parameter of interest (as with commonly used potentiometric dyes) the signal can be inverted.

3.4.2. For spatial filtering, select **Gaussian** or **Average** from the kernel menu. The size of the spatially averaged area is controlled by the **Size** input adjacent to the **Kernel** dropdown menu (i.e. 3 results in 3 pixel x 3 pixel filter kernel). When applying a Gaussian filter, the standard deviation can also be set from the **Sigma** input.

3.4.3. For baseline correction, select Top-hat[24] or polynomial (4^{th} or 11^{th} degree) correction[25] from the **Baseline** menu. Correction can be applied to each pixel individually (long processing time) or as an average of the entire image (quicker but assumes homogenous baseline alterations). Top-hat correction can also be modified by setting the **Top-Hat Length** in milliseconds, adjacent to the baseline selection dropdown menu. The length of the Top-Hat kernel should be greater than the timescale of the individual action potentials/calcium transients.

3.4.4. For temporal filtering, select Savitzky-Goaly or infinite impulse (IIR) filtering from the **Filtering** menu.

NOTE: Other than for the tissue averaged signal that appears in the bottom left, temporal filtering is applied to each pixel individually at time of parameter quantification from ensemble averaged image ranges. This has been implemented to reduce processing time by filtering small sections of data when required rather than entire files.

3.4.5. For frame removal, note that if the **Remove Frames** option is selected, large peaks with amplitude greater than the signal of interest can be removed from the image set. This may be useful in optically paced datasets such as optogenetic pacing where depolarization is initiated by optical activation of opsins such as channelrhodopsin 2[11,12].

NOTE: As frame removal will potentially introduce unphysiological step changes into the image signals, temporal filtering may introduce artifacts to the data and so is not recommended here.

3.5. Note that signal will be segmented once **Process Images** has been selected according to the options under **Segmentation options**, however this can quickly be changed without reprocessing the entire dataset (see section 4).

4. Data segmentation and ensemble averaging

NOTE: Once the file has been processed, peaks in the tissue averaged signal (bottom right trace, **Figure 1A**) will have been detected and labelled by red circles. Only peaks above a set threshold (blue line on trace that is set by **Peak Threshold**) are counted. Additionally, peaks are only

counted if they are sufficiently delayed compared to the previous peaks, set by the **Min Peak Distance** input. Signal is then segmented based on the detected peaks. First, the effective cycle length (CL) of each peak is calculated by measuring the time between it and the next peak. If a number of peaks (set by **Min Number of Peaks** input) have similar CLs (threshold for which is set by **Minimum Boundary** input) then they are grouped and the average CL for those peaks calculated.

4.1. For further segmentation of the data, press **Segment Signal**. Sub-segmentation options are: **None** – all peaks with same CL grouped together; **All** – Segments of n_{peaks} within the constant CL times (n_{peaks} is set by the **Segment size** input) are identified; **Last** – Final n_{peaks} before a CL change are identified and grouped, and all others are not analyzed; and **Single Beat** – This is equivalent to applying the **All** segmentation with $n_{peaks} = 1$, and so no grouping or ensemble averaging (see 4.5) are applied. This can be applied by selecting the **Single Beat** button.

4.1.1. Apply custom segmentation of the signal by zooming in on a time of interest and selecting **Segment Signal**. This will add an additional option entitled **Zoomed Section** to the section list box, corresponding to the time points selected.

4.2. The results of the segmentation will appear in the list-box adjacent to the tissue averaged signal, and will show section number and the estimated CL. All segmented time sections are denoted by different colors. Select a segment from the list-box to highlight that section in red. This will also automatically trigger analyses of this section, as if the **Produce Maps** button was selected (see section 5).

4.3. Analyses of grouped peaks will be performed on the 'ensemble averaged' data. This involves averaging the peaks in a segment together, with the reference times being the peaks identified in step 4.2. Update the time window to average by modifying the **before** and **after** inputs and pressing **Segment Signal**.

5. Action potential/calcium transient duration and conduction velocity analysis

5.1. Once images have been processed, the **Produce Maps** button will become active. Press **Produce Maps** to apply action potential duration (APD), activation time, conduction velocity and SNR analysis. By default, the analysis will be applied to the first signal segment. Select other segments from the list-box will apply analysis to chosen segment.

NOTE: Results of analysis are displayed in results table, including mean, standard deviation, standard error, variance and 5th to 95th percentile analysis. Duration maps are termed 'APD' maps however, calcium signals processed using the same settings will measure calcium transient duration.

5.2. Select **Get Pixel Info** to see a detailed display of the signal from any pixel within the image, and **Compare Pixels** to simultaneously plot signals from up to 6 locations.

5.2.1. Use the **Signal Processing** panel to adjust settings for duration analysis. These are: **Duration** – Time of percentage repolarisation/decay to measure from peak; **'APD' Baseline** – Time period of signal that is defined as reference baseline for amplitude measurements; and **'APD' Start time** – Start time for duration measurements. These are the same options for deciding the activation time for isochronal maps (discussed below) and are termed: Start (d^2F/dt^2_{max}), Upstroke (dF/dt_{max}), Depolarisation midpoint (time of 50% amplitude), Peak (time of maximum amplitude). These definitions applied to mouse and guinea pig action potentials are shown in **Figure 2A**.

NOTE: Changing any of these options will automatically update the duration map and the results table. Map scale and outlier removal options are also available.

5.3. Conduction velocity is also measured automatically within the main software interface. This is achieved using the multi-vector method of Bayly et al[26] from the isochronal map defined by the chosen activation measure (discussed in step 5.4). Press **Activation Points** to render a 3D representation of the activation map.

5.4. The multi-vector conduction velocity measurement method spatially segments the isochronal map into regions of *n* x *n* pixels. Set the value of *n* using the **Local Window Size** input, and set the range of activation times to apply analysis to using the **Fitting activation times** inputs.

NOTE: For each local region, a polynomial surface, f, is fitted that best describes the relationship between activation time and spatial position, (x,y). The gradient vector, CV_{local}, of this surface is then calculated as:

$$CV_{local} = \nabla f(x,y) \quad (1)$$

where ∇ denotes the two-dimensional cartesian spatial differential operator[26].

5.5. For each pixel in the isochronal map, a local vector representing speed and direction of conduction is calculated. Select **Isochronal Map with vectors** from the display dropdown menu to view this analysis.

5.6. SNR is calculated as the ratio of the maximum amplitude compared to the standard deviation of the signal at baseline. This analysis is performed post all processing steps. Press **SNR calculation** in the top menu to edit settings for the period of the signal defined as baseline.

6. Conduction analysis module

6.1. Press **Conduction** to accesses more detailed analysis of conduction velocity. This opens a separate module where conduction can be quantified using the Bayly multi-vector method as in the main interface, single vector methods, and as an activation curve.

6.2. Press **Single Vector** to analyze conduction using the single vector method, where CV is

calculated from the delay in activation time between two points. This can be done using **Automatic** or **Manual** methods, selectable below the **Single Vector** button.

6.2.1. For automatic single vector method, select a distance and start point from which to measure conduction. The software will then perform a 360-degree sweep from the selected point, measuring the time delay and calculating the associated conduction velocity along all directions in 1-degree increments. The results of this analysis are displayed in the graph adjacent to the map, and the direction of slowest conduction is shown in red.

6.2.2. For manual single vector method, choose both a start and end point from the isochronal map to calculate conduction velocity. To select a new start point, press **Clear Start Point**.

6.3. Press **Local Vector** to apply the multi vector method, with the settings matching those from the main interface. Within the conduction module, the distribution of conduction speeds, as well as the angular distribution of calculated vectors and angular dependence of conduction speed can be displayed.

6.4. Press activation curve to plot the percentage of tissue activated as a function of time. Time to 100% activation is automatically displayed, while custom values for minimum (blue) and maximum (red) activation percentages between which to measure can also be selected.

7. Additional analyses and modules

7.1.1. Aside from automatically performed duration and conduction velocity analyses, several other parameters can be quantified using ElectroMap. These analyses are selectable from the dropdown menu above the display map. Select one of these options to perform the analysis, and the results will appear in the 4th row of the results table: 1) **Diastolic Interval** – Time from 90% repolarization to activation time of the next action potential; 2) **Dominant Frequency** – Frequency spectrum of each pixel is calculated using the fast Fourier Transform, and the frequency with the most power is defined as the dominant frequency. Advanced range and window settings for dominant frequency analysis are available by selecting **Frequency Mapping**; 3) **Time to peak** – The rise time between two user selected percentages (default 10 to 90%) of the depolarization phase of the action potential or the release of calcium. Percentage values can be changed by selecting **TTP Settings**; and 4) **Relaxation constant** (**τ**) – Relaxation constant is calculated by fitting a mono-exponential decay of the form of the form:

$$F(t) = F_0 e^{-t/\tau} + C \quad (2)$$

7.2. where the fluorescence level at time t depends on the peak fluorescence, F_0, and the subsequent decay (C is a constant)[27]. The value between which to fit equation 2 are selectable within the main ElectroMap user interfaces, as well as a goodness of fit exclusion criteria based on the r^2 value.

7.3. Press **Single File Analysis** to open a dedicated module for high-throughput duration and

conduction analysis of each identified segment in a file. Analysis can be performed on either the whole image (duration, conduction and activation time) or on selected regions or points of interest (currently duration only). Results are outputted to a .csv file.

NOTE: For APD values from the whole image, the first column in the .csv file is the mean, while the second column is the standard deviation.

7.4. Press **Alternans** to initiate a standalone module for dedicated analysis and mapping of beat-to-beat variability. See O'Shea et al. 2019[13] for details on alternans processing and analysis options. Specifically, this module is designed to identify two period oscillations, known as alternans. Both duration and amplitude alternans are calculated and outputted.

NOTE: Duration alternans are measured by comparing the duration measurement from one peak to the next; i.e. if peak one and two and APD_1 and APD_2 respectively, then the duration alternan (ΔAPD) is calculated as

$$\Delta APD = |APD_1 - APD_2| \quad (3)$$

The duration measurement is performed using the settings in the main interface. Meanwhile, amplitude alternans can be quantified and mapped across multi-cellular preparations as absolute change (defined as a percentage where 0% = same amplitude between one beat and the next). Furthermore, the effects of phenomena such as calcium load can be further investigated by measuring and comparing **Load** and **Release** alternans, as has been previously reported[28]. If *L* is defined as the peak amplitude of the large beats (i.e. where the amplitude is greater than the previous beat), *S* the amplitude of the small beats, and *D* the diastolic load of the small beats, the release alternans ($ALT_{release}$) are defined as:

$$ALT_{release} = 1 - (S/L) \quad (4)$$

Conversely, load alternans (ALT_{load}) are defined as:

$$ALT_{load} = D/L \quad (5)$$

Alternans measurements can be made across the whole tissue, and the results of the analysis are displayed in the bottom right of the module. When first using the module, the analysis is performed across the entire experimental file, and the results displayed are an average beat-beat difference across the whole file. However, analysis can be restricted to specific times in the file by de-selecting **Hold Zoom**, zooming in on a specific time period, and selecting **Analyse Zoomed Section**. This will update the results panel to show analysis from the selected time period.

7.4.1. Select play to show a beat-to-beat video of the alternans analysis. Additionally, select **Create Mean Map** to export a map of the alternans behavior averaged from the selecting time points, which are set in the pop-up menu when using this feature.

7.5. Press **Phase Map** to initiate the phase mapping module. A Hilbert transform is performed to calculate the instantaneous phase (between -π and +π) of the signals at each timepoint. Press play or drag slider to visualize phase behavior over time and click on a pixel to render a phase diagram.

8. Exporting data

8.1. Data is exported from ElectroMap in a variety of forms. Press **Export Values** to save the values of the currently displayed map in the main used interface. Measured values can be saved as either a map (preserving pixel locations) or condensed into a single list, and can be saved as .csv,.txt or .MAT files.

8.2. Press **Export Map** to bring up a pop-up containing the currently displayed map, which can then be saved in a variety of image formats. Display options for the map are controlled by selecting **Map Settings** but can also be edited once **Export Map** has been selected. For example, a color bar can be added by selecting this icon from the top menu, and the scale can be set by selecting **Edit** > **Colormap**.

8.3. Press **Activation Video** to render an animation of the activation sequence, which can be saved as an animated .gif file.

8.4. Press **Segment Video** to save a .avi video file of the currently displayed parameter of each identified segment.

REPRESENTATIVE RESULTS:

All work performed as part of this study was undertaken in accordance with ethical guidelines set out by the UK Animals (Scientific Procedures) Act 1986 and Directive 2010/63/EU of the European Parliament on the protection of animals used for scientific purposes. Experiments were approved by the home office (mouse: PPL 30/2967 and PFDAAF77F, guinea pig: PPL PF75E5F7F) and the institutional review boards at University of Birmingham (mouse) and King's College London (guinea pig). Detailed methods for collection of the raw data that has been analyzed here can be found in our previous publications[5,6,14,19].

The main interface from which ElectroMap is controlled is shown in **Figure 1A**. The necessary steps to analyze a dataset are controlled primarily by the **Load Images**, **Process Images**, and **Produce Maps** buttons, and are shown highlighted in green, blue, and red, respectively in **Figure 1A**. **Figure 1B–D** show the operations that occur on selection of each of these buttons. **Load Images** applies the image thresholding options as selected by the user (**Figure 1B**), while **Process Images** (**Figure 1C**) applies filtering and baseline correction. Finally, **Produce Maps** will first average data according to the time window and segmentation settings (unless single beat segmentation is chosen) and then perform analyses described above.

A key aspect of ElectroMap is its flexibility with respect to camera type and experimental model.

This is crucial for the utility of an optical mapping software due to the distinct cardiac EP and anatomical characteristics that exist between widely used models. **Figure 2A** for example shows the action potential morphology of the murine atria when compared to the guinea pig ventricle, recorded using voltage sensitive dyes as previously reported[6,14]. Despite the distinct shape of the action potential, and the use of two separate optical mapping cameras with different framerates and pixel sizes, ElectroMap can be utilized to successfully analyze both datasets. However, this requires modification of some parameters within the user interface (**Figure 2B**). Note that the prolonged guinea pig action potential necessitates a larger time window. Additionally, to prevent top-hat baseline correction unphysiologically modifying the optically recorded signals, its time length must be increased so that it is greater than the time course of the action potential.

ElectroMap offers a multitude of processing options to help improve the SNR of optically recorded signals which may be required to effectively recover EP parameters. An example is automated ensemble averaging of peaks following data segmentation. **Figure 3A–C** demonstrates how the application of ensemble averaging, in lieu of other methods, can improve SNR from isolated murine left atria (*n* = 13). This reduces measurement heterogeneity and likelihood of analysis failure (**Figure 3D**). For example, a change of pacing frequency from 3 Hz to 10 Hz did not alter APD_{50}, when no ensemble averaging is undertaken, yet an expected[29] decrease in APD_{50} at 10 Hz pacing was observed when measured from ensemble averaged data (**Figure 3E**).

Figure 4 demonstrates the efficacy and utility of automated pacing frequency detection and segmentation offered by ElectroMap. Here, mouse left atria (n = 5) were paced at a 120 ms cycle length and cycle length was incrementally shortened by 10 ms until it reached 50 ms. ElectroMap automatically identified the pacing cycle length and grouped tissue averaged peaks accordingly (**Figure 4A**). This was achieved with high accuracy in all datasets (**Figure 4B**). Automated segmentation of the data allowed straightforward and high throughput analysis of the slowing of conduction velocity with increased pacing frequency/shortened cycle length (**Figure 4C,D**). Concurrently, APD_{50} (**Figure 4E**) and diastolic interval (**Figure 4F**) shortened. Amplitude of the optically measured peaks decreased, while time to peak increased **(Figure 4G,H**). These are again the expected restitution responses in cardiac tissue[29,30] and use of ElectroMap can help therefore elucidate changes in response to pacing frequency in presence of pharmacological agents, genetic modification, or disease states.

An important consideration in the use of a software such as ElectroMap is the presence of artifacts in the underlying data. **Figure 5**, for example demonstrates that motion artifacts (the distortion of the optically recorded signal by tissue movement) can preclude accurate measurements of activation and especially repolarization within ElectroMap. See Discussion for further considerations.

FIGURE AND TABLE LEGENDS:

Figure 1: ElectroMap main processing steps. (**A**) Graphical user interface of ElectroMap, with the **Load Images** (green), **Process Images** (blue), and **Produce Maps** (red) buttons highlighted. (**B**)

Image thresholding options that can be applied on selecting **Load Images**. (**C**) Signal processing options available to the user include spatial and temporal filtering and baseline correction and can be applied to the image stack by pressing **Process Images**. (**D**) Ensemble averaging and parameter quantification (shown APD measurement) that is activated by selecting **Produce Maps**. Figure adapted from O'Shea et al., 2019[13].

Figure 2: Analysis of mouse and guinea pig data using ElectroMap. (**A**) Optically recorded action potential from mouse atria and guinea pig ventricles, along with both the first (df/dt) and second (d^2f/dt^2) derivate of these signals. The various definitions for activation and repolarization times employable within ElectroMap are highlighted. (**B**) Screenshots of Image and signal processing settings utilized in ElectroMaps interface. Red boxes highlight settings that required modification between analyses of mouse and guinea pig data. Figure adapted from O'Shea et al., 2019[13].

Figure 3: Ensemble averaging to resolve APD changes. (**A**) APD_{50} map and example single pixel signal from single beat optical action potentials. (**B**) APD_{50} map and example single pixel signal from optical action potentials generated by ensemble averaging of 10 successive beats (peak method). (**C**) SNR of single beat compared to 10 beat averaged signals. (**D**) APD_{50} heterogeneity (i) and number of measurement failures (ii) as a function of SNR for single beat and 10 beat averaged APD_{50} maps. (**E**) APD_{50} at 3 and 10 Hz pacing frequency, as measured from single beat and 10 beat maps. (Data shown as mean ± standard error, n = 13 left atria, ****$p < 0.001$ by student's paired t-test).

Figure 4: Use of ElectroMap to study pacing frequency responses in cardiac tissue. (**A**) Example ElectroMap screenshot of pacing frequency recognition and segmentation. (**B**) Comparison of known and ElectroMap measured pacing cycle lengths. (**C**) Activation maps at 120 ms and 60 ms pacing cycle lengths. (**D–H**) Grouped data of conduction velocity (**D**), APD_{50} (**E**), diastolic interval (**F**), amplitude (**G**), and time to peak (**H**) as a function of pacing cycle length decreasing from 120 ms to 60 ms in 10 ms increments. (Data shown as mean ± standard error, n = 5 left atria)

Figure 5. Effect of motion artifacts. (**A**) APD_{50} map. (**B**) Activation map. (**C**) Example signals from locations marked (crosses) on APD and activation maps. In the area of the tissue marked with the red cross, contraction has not been successfully uncoupled, distorting the measured optical signal.

DISCUSSION:

Here, we present a step-by-step guide for the utilization of open-source software ElectroMap for flexible and multi variable analysis of cardiac optical mapping datasets. For successful use of ElectroMap, imaging data is required to be in .tif or .MAT formats. ElectroMap incorporates several modifiable user settings. As demonstrated in **Figure 2A**, this is necessary due to the wide heterogeneity that exists between experimental models and imaging hardware. This means however that default settings within the software will not always be optimal, so a critical step in using the software is for the user to tune settings for their particular experimental setup. These include camera settings and timescales, as shown in **Figure 2B**. Once optimal settings have been

found, these can be saved and reloaded at later times by selecting **Configuration File**.

Incorporation of automated CL measurement and signal segmentation are key advantages of the software. These features allow analysis of acute responses in experimental recordings and widen analysis from focusing on isolated single beats. Once desired segmentation has been achieved, the **Single File Analysis** module allows automated analysis of each individual segment (including single beats), realizing high-throughput analysis of multiple variables across the recording outputted in a single .csv file. In conjunction, ensemble averaging of grouped peaks is an effective method to improve quality of noisy signals that is automatically performed in ElectroMap. However, ensemble averaging is not ubiquitously beneficial, for example in studies of beat-to-beat variability. Therefore, ElectroMap integrates single beat segmentation to avoid ensemble averaging, alternative processing options to improve SNR (spatial and temporal filtering) and includes the **Alternans** analysis module to further investigate and map beat-to-beat variability.

Optical Mapping datasets often exhibit artifacts such as baseline drift and motion artifacts. Equally, the signals generated can be low quality due to small pixel sizes, short exposure times and low fractional fluorescent changes[2]. These factors prevent effective and accurate analysis of the underlying EP behavior. As outlined, ElectroMap has several processing strategies to overcome these issues. However, application of these algorithms to fundamentally poor quality/distorted data will still prevent effective analysis. SNR is therefore one of the parameters that is measured and displayed in ElectroMap. Equally, the user can select and compare the signals from specific regions from the sample using the **Pixel Info** and **Compare** modules, allowing identification of phenomena such as motion artifacts shown in **Figure 5**, and appropriate exclusion of data.

At present, ElectroMap does not support removal of motion artifacts from raw data in the same manner as baseline correction. Therefore, a possible future development of the software is inclusion of motion artefact removal by computational methods as has been reported[31,32]. Furthermore, ElectroMap is currently limited to study of one optical signal. However, for ratiometric dyes and simultaneous use of voltage and calcium dyes[27], concurrent processing of two wavelength channels is required. The integration of dual signal analysis is therefore an important future addition to the software. Extension of analysis options applicable to arrhythmic datasets, such as phase singularity tracking, would equally broaden the scope of the software[33,34]. Finally, several of the analysis options described can also be useful in analysis of the electrode mapping data. Indeed, ElectroMap has been used to analyze electrode mapping data despite the contrasting electrogram waveform[20,35], and further optimization will expand its use for this modality.

ACKNOWLEDGMENTS:

This work was funded by the EPSRC studentship (Sci-Phy-4-Health Centre for Doctoral Training L016346) to D.P., K.R. and L.F., Wellcome Trust Seed Award Grant (109604/Z/15/Z) to D.P., British Heart Foundation Grants (PG/17/55/33087, RG/17/15/33106) to D.P., European Union (grant agreement No 633196 [CATCH ME] to P.K. and L.F.), British Heart Foundation (FS/13/43/30324

to P.K. and L.F.; PG/17/30/32961 to P.K. and A.H.), and Leducq Foundation to P.K.. J.W. is supported by the British Heart Foundation (FS/16/35/31952).

DISCLOSURES:

P.K. receives research support from several drug and device companies active in atrial fibrillation and has received honoraria from several such companies. L.F. has received institutional research grants EU, BHF, MRC, DFG and Gilead. P.K. and L.F. are listed as inventors on two patents held by University of Birmingham (Atrial Fibrillation Therapy WO 2015140571, Markers for Atrial Fibrillation WO 2016012783).

All other authors declare no potential conflict of interest.

REFERENCES:

1. Efimov, I. R., Nikolski, V. P., Salama, G. Optical Imaging of the Heart. *Circulation Research.* **94,** 21–33 (2004).
2. Herron, T. J., Lee, P., Jalife, J. Optical imaging of voltage and calcium in cardiac cells & tissues. *Circulation Research.* **110,** 609–623 (2012).
3. Boukens, B. J., Efimov, I. R. A century of optocardiography. *IEEE Reviews in Biomedical Engineering.* **7,** 115–125 (2014).
4. Myles, R. C., Wang, L., Kang, C., Bers, D. M., Ripplinger, C. M. Local β-adrenergic stimulation overcomes source-sink mismatch to generate focal arrhythmia. *Circulation Research.* **110,** 1454–1464 (2012).
5. Syeda, F. et al. PITX2 Modulates Atrial Membrane Potential and the Antiarrhythmic Effects of Sodium-Channel Blockers. *Journal of the American College of Cardiology.* **68,** 1881–1894 (2016).
6. Winter, J. et al. Sympathetic nervous regulation of cardiac alternans in the intact heart. *Frontiers in Physiology.* **9,** 1–12 (2018).
7. Faggioni, M. et al. Suppression of spontaneous ca elevations prevents atrial fibrillation in calsequestrin 2-null hearts. *Circulation: Arrhythmia and Electrophysiology.* **7,** 313–320 (2014).
8. Sato, P. Y. et al. Loss of Plakophilin-2 Expression Leads to Decreased Sodium Current and Slower Conduction Velocity in Cultured Cardiac Myocytes. *Circulation Research.* **105,** 523–526 (2009).
9. Yu, T. Y. et al. Optical mapping design for murine atrial electrophysiology. *Computer Methods in Biomechanics and Biomedical Engineering: Imaging & Visualization.* **5,** 368–378 (2017).
10. Laughner, J. I., Ng, F. S., Sulkin, M. S., Arthur, R. M., Efimov, I. R. Processing and analysis of cardiac optical mapping data obtained with potentiometric dyes. *American Journal of Physiology. Heart and Circulatory Physiology.* **303,** H753-65 (2012).
11. Crocini, C., Ferrantini, C., Pavone, F. S., Sacconi, L. Optogenetics gets to the heart: A guiding light beyond defibrillation. *Progress in Biophysics and Molecular Biology.* **130,** 132–139 (2017).

12. Entcheva, E., Bub, G. All-optical control of cardiac excitation: Combined high-resolution optogenetic actuation and optical mapping. *The Journal of Physiology.* **9,** 2503–2510 (2016).
13. O'Shea, C. et al. ElectroMap: High-throughput open-source software for analysis and mapping of cardiac electrophysiology. *Scientific Reports.* **9,** 1–13 (2019).
14. Yu, T. Y. et al. An automated system using spatial oversampling for optical mapping in murine atria. Development and validation with monophasic and transmembrane action potentials. *Progress in Biophysics and Molecular Biology.* **115,** 340–348 (2014).
15. Jaimes, R. et al. Functional response of the isolated, perfused normoxic heart to pyruvate dehydrogenase activation by dichloroacetate and pyruvate. *Pflugers Archiv.* **468,** 131–142 (2016).
16. Wang, K. et al. Cardiac tissue slices: preparation, handling, and successful optical mapping. *American Journal of Physiology. Heart and Circulatory Physiology.* **308,** H1112-25 (2015).
17. Parrish, D. C. et al. Transient denervation of viable myocardium after myocardial infarction does not alter arrhythmia susceptibility. *American Journal of Physiology. Heart and Circulatory Physiology.* doi:10.1152/ajpheart.00300.2017 (2017).
18. Ihara, K. et al. Electrophysiological Assessment of Murine Atria with High-Resolution Optical Mapping. *Journal of Visualized Experiments.* **132,** e56478 (2018).
19. Holmes, A. P. et al. A Regional Reduction in Ito and IKACh in the Murine Posterior Left Atrial Myocardium Is Associated with Action Potential Prolongation and Increased Ectopic Activity. *Plos One.* **11,** e0154077 (2016).
20. Lang, D. et al. Arrhythmogenic remodeling of β<inf>2</inf> versus β<inf>1</inf> adrenergic signaling in the human failing heart. *Circulation: Arrhythmia and Electrophysiology.* **8,** 409–419 (2015).
21. Kang, C. et al. Human Organotypic Cultured Cardiac Slices: New Platform For High Throughput Preclinical Human Trials. *Scientific Reports.* **6,** 1–13 (2016).
22. Wen, Q. et al. Transverse cardiac slicing and optical imaging for analysis of transmural gradients in membrane potential and Ca2+ transients in murine heart. *The Journal of Physiology.* **596,** 3951–3965 (2018).
23. Houston, C. et al. Characterisation of re-entrant circuit (or rotational activity) in vitro using the HL1-6 myocyte cell line. *Journal of Molecular and Cellular Cardiology.* **119,** 155–164 (2018).
24. Yu, T. Y. et al. Optical mapping design for murine atrial electrophysiology. *Computer Methods in Biomechanics and Biomedical Engineering: Imaging and Visualization* **5,** 368–376 (2017).
25. Laughner, J. I., Ng, F. S., Sulkin, M. S., Arthur, R. M., Efimov, I. R. Processing and analysis of cardiac optical mapping data obtained with potentiometric dyes. *AJP: Heart and Circulatory Physiology.* **303,** H753–H765 (2012).
26. Bayly, P. V et al. Estimation of Conduction Velocity Vector Fields from Epicardial Mapping Data. *IEEE Transactions on Bio-Medical Engineering.* **45,** 563–571 (1998).
27. Jaimes, R. et al. A technical review of optical mapping of intracellular calcium within myocardial tissue. *American Journal of Physiology. Heart and Circulatory Physiology.* **310,** H1388–H1401 (2016).
28. Wang, L. et al. Optical mapping of sarcoplasmic reticulum Ca2+ in the intact heart:

Ryanodine receptor refractoriness during alternans and fibrillation. *Circulation Research.* **114,** 1410–1421 (2014).
29. Winter, J., Shattock, M. J. Geometrical considerations in cardiac electrophysiology and arrhythmogenesis. *Europace.* doi:10.1093/europace/euv307 (2016).
30. Mironov, S., Jalife, J., Tolkacheva, E. G. Role of conduction velocity restitution and short-term memory in the development of action potential duration alternans in isolated rabbit hearts. *Circulation.* **118,** 17–25 (2008).
31. Khwaounjoo, P. et al. Image-Based Motion Correction for Optical Mapping of Cardiac Electrical Activity. *Annals of Biomedical Engineering.* **43,** 1235–1246 (2014).
32. Christoph, J., Luther, S. Marker-Free Tracking for Motion Artifact Compensation and Deformation Measurements in Optical Mapping Videos of Contracting Hearts. *Frontiers in Physiology.* **9,** (2018).
33. Umapathy, K. et al. Phase Mapping of Cardiac Fibrillation. *Circulation: Arrhythmia and Electrophysiology.* **3,** 105–114 (2010).
34. Tomii, N. et al. Detection Algorithm of Phase Singularity Using Phase Variance Analysis for Epicardial Optical Mapping Data. *IEEE Transactions on Biomedical Engineering.* **63,** 1795–1803 (2016).
35. Cantwell, C. D. et al. Techniques for automated local activation time annotation. and conduction velocity estimation in cardiac mapping. *Computers in Biology and Medicine* **65,** (2015).